RESPONSE AND STRENGTH OF LAMINATES UNDER THERMOMECHANICAL LOADS

A thesis submitted
in partial fulfillment of the requirements
for the degree of

MASTER OF TECHNOLOGY

by

Siju Samuel

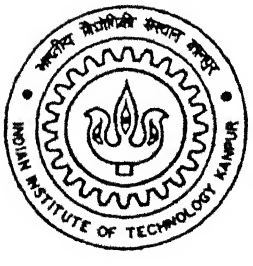

to the

DEPATMENT OF CIVIL ENGINEERING
INDIAN INSTITUTE OF TECHNOLOGY, KANPUR

September, 1999

CERTIFICATE

It is certified that the work contained in the thesis entitled **Response and Strength of Laminate Under Thermomechanical Loads,** by Siju Samuel, has been carried out under my supervision and that this work has not been submitted elsewhere for a degree.

September, 1999

Ashwini Kumar
Professor
Department of Civil Engineering
Indian Institute of Technology Kanpur

be sincere

be straightforward

Dedicated to my parents, sister

and all those who have cared me inside.....

ACKNOWLEDGEMENTS

I have great pleasure in expressing my heartful gratitude to my thesis supervisor Prof. Ashwini Kumar, for his valuable and sincere guidance during the entire course of this work. It has been a peaceful and pleasant experience to work with him. And, I am very thankful to him for being with me through my tough times. Also, I am grateful to all my professors who sincerely wished for my betterment.

IIT-K is a different world. The lectures, seminars, friends, functions, times at library and in reading room – all have been splendid experiences.

It is too nice to tell, it is quite easy to have friendships in this place of learning. Roshan, Nishanth and Davidettan are too special for me. It has been too good to talk with Abhi, Babu and Sreejith. Thanks to Jinu, Jibu, Shibu, Roy, Jacob, Jayan, Kutty and Nahas for making those pleasant evenings. Also, I extend my thanks to my seniors Maymol, Prince, Murali, George, Ajith, Biju, Balu and Satheesh for the intimacy and care I have received. I must single out Prof. Joseph John and his family for their helpful presence.

I am thankful to Ranjith, Naram and P.N. Jha for giving me the help and the right support in all academic matters. Thanks to all classmates for the friendship and cooperation.

From my heart deep, I am indebted to my papa, mummy, sister and appachan for their constant support and good will. I am greatly obliged to all my teachers and friends I had in my study life. I am so thankful to every one who gave me the real human care. I always like to think that my small achievements are due to their good wishes.

IIT-K has been a world with beautiful tensions and positive thinking, where one can do work for a better tomorrow. In my nostalgic memories, I would be proud in keeping those moments in this temple of worship, so close to my heart.

IIT Kanpur *Siju*

Semptember, 1999

ABSTRACT

A study is made of post-buckling response and first-ply failure of flat unstiffened fibrous composite laminates subjected to uni-axial compression and a uniform temperature field. The analysis is based on the first-order shear deformation von-Karman type nonlinear plate theory. An efficient finite element formulation based on the principle of minimum potential energy is used for determining response characteristics, in conjunction with the first-ply failure analysis based on Tsai-Wu criterion. The main task is to obtain the stability boundary and the first-ply failure envelope for symmetric laminates having five different types of lay-up. The influence of temperature dependent thermo-mechanical material properties on the response of laminates is also investigated.

CONTENTS

Acknowledgements iv

Abstract v

Contents vi

List of Figures viii

List of Tables x

Nomenclature xi

1 Introduction 1

1.1 Composite Materials 1

1.2 Literature Review 3

1.3 Aim of Present Investigation 5

2 Finite Element Formulation and Failure Model 7

2.1 Introduction 7

2.2 Plate Deformation, Strains and Stress-Strain Relations.....7

2.3 Stress Resultants at the Mid-Plane of the Laminate.....9

2.4 Total Langrangian and Virtual Work Equation 11

2.5 Finite Element Formulation 13

2.5.1 First-variation of total in-plane strain 14

2.5.2 First-variation of bending strain 16

2.5.3 First-variation shear strain 17

2.5.4 Equivalent nodal load vector 17

2.5.5 Non-linear equilibrium equation 18

2.6 Solution of Non-linear Equilibrium Equation 18

2.7 Failure Criteria 20

3 Numerical Results and Discussion **22**

3.1 Convergence and Validation Study 22

3.2 Analysis Details 23

3.3 Numerical Studies 27

3.3.1 Thermal post-buckling response 27

3.3.2 Stability envelope 28

3.3.3 First-ply failure envelope 29

3.4 Parametric study: effect of number of layers 37

4 Concluding Remarks **39**

References **41**

Appendix I **45**

Appendix II **47**

LIST OF FIGURES

2.1 Geometry of a NL layered laminate 9

2.2 Edge traction 12

3.1 Convergence and validation of solution 23

3.2 Verification of solution under combined loading 24

3.3 Details of geometry and boundary conditions and sign conventions for stress resultants and generalized displacement. 25

3.4 Element and node numbering scheme for laminated plates 27

3.5 Response of $(\pm 45/0/90)_{2s}$ laminate considering thermal dependent (TD) and independent (TID) material properties 28

3.6 Stability envelope for $(\pm 45/0/90)_{2s}$ laminate considering thermal dependent (TD) and independent (TID) material properties 29

3.7 Stability envelopes considering thermal dependent (TD) and independent (TID) material properties 30

3.8 Stability and failure envelopes for $(+45/-45/0/90)_{2s}$ laminate considering thermal dependent (TD) and independent (TID) material properties 30

3.9 First-ply failure envelopes considering thermal dependent (TD) and independent (TID) material properties 31

3.10 Transverse deflection for $(45/-45/0/90)_{2s}$ under combined loading at different temperature interval 32

3.11a Edge displacement under axial compression at x = 0, node 56. 33

3.11b Edge displacement under temperature rise at x = 0, node 56 33

3.12a Variation of stress σ_x at node 1, layer 2 34

3.12b Variation of stress τ_{xy} at node 1, layer 2 35

3.12c Variation of stresses under temperature rise at node 1, layer 2 35

3.13a Variation of stress σ_x at node 1, layer 15 36

3.13b Variation of stress τ_{xy} at node 1, layer 15 36

3.13c Variation of stresses under temperature rise at node 1, layer 15 37

3.14 First-ply failure envelopes for $(45/-45/0/90)_{ns}$ laminates

under combined loading 38

LIST OF TABLES

3.1 Composite panels considered 24

3.2 Material mechanical properties 26

3.3 Material strength properties 26

NOMENCLATURE

a, b, h	Dimensions of the plate along x, y and z coordinate directions
C_{ij}	Elastic constants of a lamina in the principal material directions
E_i	Young's moduli along the principal material directions
G_{ij}	Shear moduli in three orthogonal principal planes
K_T	Tangent stiffness matrix
K_L, K_{NL}, K_σ	Linear, nonlinear and initial component matrices of tangent stiffness matrix
k_1, k_2	Shear correction factors
M_x, M_y, M_{xy}	Bending stress resultants per unit length
$\overline{M}_x, \overline{M}_y, \overline{M}_{xy}$	Thermal moment resultants per unit length
N	Number of nodes per element
NL	Number of layers of laminated plate
N_I, $(I = 1,N)$	Shape function
N_x, N_y, N_{xy}	In-plane stress resultants per unit length
$\overline{N}_x, \overline{N}_x, \overline{N}_{xy}$	Thermal force resultants per unit length
p_n, p_t	Local edge tractions per unit area
p_x, p_y	Global edge tractions per unit area
Q_x, Q_y	Transverse shear stress resultants
q	Transverse force per unit area
R	Equivalent nodal load vector
R'	Shear strength of the lamina in plane 2-3

$\nu_{12}, \nu_{13}, \nu_{23}$	Poisson's ratios in planes 1-2, 1-3 and 2-3 , respectively
ΔT	Rise in temperature
$\{K\}$	Bending strain vector
$\{a_i\}$	Displacement of the i^{th} node
$\{\varepsilon_p^0\}$	In-plane strain vector
$\{\varepsilon_s^0\}$	Transverse shear strain vector
$\{\varepsilon^0\}^l$	Linear component of in-palne strain vector
$\{\varepsilon^0\}^{nl}$	Nonlinear component of in-palne strain vector
$\psi\{a\}_i$	Residual (unbalanced) force vector
$\Delta\{a\}_i$	Incremental displacements at the end of the i^{th} iteration
$[A]$	Extensional matrix
$[B]$	Extension-bending coupling matrix
$[D]$	Bending stiffness matrix
$[E]$	Transverse shear stiffness matrix
$\delta(\ )$	First-variation of a quantity
$\frac{\partial}{\partial x}(\ )$	Partial derivative of a variable with respect to x
$\frac{\partial}{\partial y}(\ )$	Partial derivative of a variable with respect to y
$\frac{\partial}{\partial z}(\ )$	Partial derivative of a variable with respect to z

S	Shear strength of the lamina in plane 1-3
T'	Shear strength of the lamina in plane 1-2
T	Temperature at the midplane of the plate
u, v, w	Displacement along x, y, z respectively of any point (x, y, z) in the plate
u_0, v_0, w_0	Mid-plane displacement in x, y and Z directions, respectively
X_t, X_c	Tensile and compressive strength, respectively, of lamina in the fiber direction
Y_t, Y_c	Tensile and compressive strength, respectively, of lamina in the direction transverse to the fiber direction
Z_t, Z_c	Tensile and compressive strength, respectively, of lamina in principal material direction-3
α	Fiber orientation measured +ve in anti-clockwise direction
α_x, α_y	Coefficients of thermal expansion with respect to the structural axis
α_1, α_2	Coefficients of thermal expansion of individual layers in direction of fibers and normal to fiber direction respectively
θ_x, θ_y	Rotation of normal to the undeformed mid-plane in xz and yz planes, respectively
$\sigma_x, \sigma_y, \tau_{xy}$	Stress components in xy plane
$\sigma_1, \sigma_2, \sigma_3$	Normal stress components in principal material directions 1,2 and 3, respectively
τ_{xz}, τ_{yz}	Transverse shear stress components in xz and yz planes, respectively
$\tau_{12}, \tau_{13}, \tau_{23}$	Shear stress components in planes 1-2, 1-3 and 2-3 respectively

CHAPTER 1

INTRODUCTION

1.1 Composite Material

Engineering sounds metallic. Metals are, by far, the most versatile engineering materials. In modern engineering structures, new composite material systems exhibiting exotic properties play a big role as compared to the traditional metallic ones.

The word "composite" refers to a material consisting of two or more chemically distinct constituents, on a macro scale, having a distinct interface separating them. In addition, the properties are strongly influenced by the properties of its constituent materials, their distribution and their mutual interaction. This definition encompasses the 'continuous fiber-reinforced laminated composites' which are of primary interest in this study.

A laminated composite comprises several layers, termed lamina, consisting of high performance fibers (e.g. glass, boron, graphite) unified by advanced binders called matrix (e.g. epoxy resin). The use of composite material in various structural applications is dictated by factors like the increased strength, stiffness, improved structural response, low maintenance cost and high service life. Because of their high strength and stiffness to weight ratios and better thermal properties, these new materials are going to play a great role in the construction of aeronautical and aerospace vehicles as well as of turbojet engines, large space structures and nuclear reactor components.

Composite structures are generally subjected to external mechanical loads, aerodynamic loads, gust loads, thermal loads, moisture loads or its combinations. A major part of the above mentioned structures are going to operate in hostile thermo-mechanical environments which could result in significant modifications in their response

characteristics. This is especially valid for supersonic space vehicles where, as a result of aerodynamic heating, the structure is exposed to a non-uniform temperature field. In view of this, the consideration of simultaneous actions of thermal and mechanical loads pose challenging technical problems in understanding the structural response, failure criteria and design of composite structures.

High performance composite laminates lead to new opportunities in the design of structures. Composite structures show flexible anisotropy and are characterized by bending-extension coupling. This gives the freedom to tailor the stiffness and strength, especially in the case of laminated filamentary composites. In contrast to an isotropic material, composite materials have a low ratio of transverse shear modulus to the in-plane modulus. Owing to this fact, the transverse shear deformation plays a much more important role in reducing the effective flexural stiffness of laminated composites plates than in the corresponding metallic plates. The laminates used in most of the structures are usually thin and in many applications, the design may require an exhaustive use of the post-buckling strength. In the presence of elevated temperature the response characteristics become more complicated. Further, in many composite materials the temperature causes significant variations in the thermal and mechanical properties. The strength and moduli of most of the materials decrease with rise in temperature, while Poisson's ratios and coefficients of thermal expansions usually increase.

Design has to make use of the above mentioned features to provide better performance advantages depending upon the functional requirements of the structure. This demands an efficient modeling.

A lamina is idealized as an orthotropic material. Plates and shell structures made of laminated composite materials are often modeled as equivalent two dimensional continuum using classical laminate theory, which is a direct extension of the Kirchoff hypothesis for homogeneous thin plates. As is well known, geometric non-linearities arise from finite deformations of an elastic body. The investigations of the response in bending, buckling and post-buckling of composite laminates is far more involved and complicated when compared to its isotropic counterpart. The von-Karman's assumptions governing large transverse deflections (of the order of thickness) for anisotropic, heterogeneous, thermoelastic thin plates are extended for the non-linear analysis of

laminated composites. For moderately thick plates, in which the effect of shear deformation can be significant, the application of the Reissner-Mindlin theory or higher order shear deformation theories becomes necessary.

It is almost impossible to look for closed form solutions for most of the practical problems involving composite laminates. The approximate analytical techniques, which have been applied to study the buckling and the post-buckling behavior of flat composite plates, are mostly limited to the cases having simple boundary conditions. Using the finite element technique, it has been possible to perform the analysis of composite laminates of complex geometry (e.g. plates with cutouts or having stiffeners), with complicated boundary conditions (e.g. elastic, discontinuous or point supports), having variable thickness and with temperature dependent material properties. The displacement finite element models, based on the principles of virtual displacement, have emerged as the most powerful tools for the solution of problems related to composite structures.

An efficient and economical design of laminates by fully exploiting their strength characteristics with high reliability and safety requires a thorough understanding of the failure mechanism. A first ply failure analysis is often used in predicting the laminate strength. Various macroscopic failure criteria based on tensile, compressive and shear strength of the individual lamina are used for this purpose. Equally important is to have the knowledge of the mode of failure and its consideration. Laminated composites may fail by fiber yielding, matrix yielding, fiber breakage, delamination of layer or by fracture.

In case of thermal problems, the elevated temperature usually lowers the matrix strength such as transverse and shear strengths, but reduces residual stresses. The static tensile strength of laminates with fiber dominant failure modes is relatively insensitive to temperature.variations.

1.2 Literature Review

A vast amount of literature is available on diverse aspects of thermoelastic response of composite laminates. A comprehensive summary of the state of art in nonlinear analysis

of bending and post-buckling of isotropic, orthotropic, anisotropic and unsymmetrically laminated plates was compiled by Chia (1988).

A survey paper by Tauchert (1991) on thermally induced flexure, buckling and vibration of plates gives an up-to-date account of buckling, post-buckling and large deformation of plates associated with elevated temperatures. The most comprehensive review paper by Noor and Burton (1991) details hierarchy of composite models, the effect of temperature dependence of the material properties on the response, and the sensitivity of thermo-mechanical load to the variations in material parameters.

During the last decade, many investigations have been done on the post buckling response of composite laminates. Huang and Tauchert (1988a, 1988b) investigated the thermal post-buckling of antisymmetric angle-ply laminated plates under uniform and parabolic temperature fields through a direct applications of the principle of minimum potential energy. A major effort in dealing with the problem of thermally induced large deflections by the finite element method was done by Chen and Chen (1989). Huang and Tauchert (1991) investigated the large deflection response of flat plates and cylindrical panels under thermal loading, using the finite element formulation based on the first order shear deformation theory. The nonlinear response of antisymmetric cross-ply laminates under the uniform temperature field was studied by Kumar and Dixit (1994).

Chen and Chen (1991) examined the effect of temperature dependent properties on thermal post-buckling behavior of laminated plates. It was found that the post-buckling strength got reduced significantly when temperature dependent properties were taken into consideration. Mayers and Hayer (1992) studied the thermal post-buckling of symmetrically laminated plates using the Raleigh-Ritz procedure. Shen and Lin (1995) considered the post-buckling response of geometrically imperfect laminates using the Galerkin perturbation technique under uniform/nonuniform temperature loading.

The buckling problem of isotropic long plates subjected to heat and axial loads was considered by Boley and Weiner (1960). Thermal buckling loads of initially compressed transversely isotropic and anti-symmetric cross-ply laminated thick plates were evaluated using the Galerkin method by Chen *et al.* (1982). The influence of uniformly elevated temperature on the buckling loads of uniaxially compressed isotropic long plates was analyzed by Sadovsky (1993). Noor and Peters (1992) made an analytical study, based

on first order shear deformation theory, for the thermo-mechanical buckling of composite plates subjected to combined thermal and axial loading. A mixed finite element method is used, for determining the stability boundary and for evaluating the sensitivity of the buckling response to variations in the material and geometric parameters. Noor *et al.* (1993) calculated the buckling load and the post-buckling response of flat unstiffened panels subjected to combined temperature change and applied edge displacement. The analysis was based on a first order shear deformation, von-Karaman type nonlinear plate theory. Numerical results were presented showing the effects of variations in the laminate stacking sequence, fiber orientation, number of layers and aspect ratio of the panels on the thermo-mechanical buckling load and the post-buckling response. Liberscu and Souza (1993) analyzed the post-buckling of an imperfect, shear- deformable, transversely isotropic plate under combined thermal and compressive edge loading. A post-buckling analysis for a simply supported, composite laminated plate resting on a two-parameter elastic foundation subjected to combined axial compression and uniform temperature loading was conducted by Shen and Sun (1996). Argyris and Tenek (1995) studied the thermo-mechanical post-buckling response of fibrous composite laminates. Temperature-dependent material properties in cubic variations were incorporated. It was found that the mechanical property degradation due to temperature rise had large influence on the response of the laminate. Srikanth (1997) studied the response and the first-ply failure of thin temperature sensitive laminated composite plates under thermal loading.

Quasi-static thermal stress response and failure behavior of graphite/epoxy laminated plate under combined thermal and mechanical loads was investigated by Chen *et al.* (1985). Effects of ablation, degradation of thermo-physical and strength properties at elevated temperature, and radiation and convective heat losses were included in the formulation. The maximum stress criterion was adopted for the failure predictions.

1.3 Aim of Present Investigation

The literature review reveals that very few investigations are available related to buckling and post-buckling behavior of composite plates subjected to combined thermal and mechanical loads. Also, studies related to the failure of composite plates under thermal

loading are rather limited in scope. In much of the earlier works, an assumption is frequently made that the material properties are temperature independent. But, temperature causes significant variation in thermal, mechanical and strength properties of the material. The accurate prediction of response requires accounting for the effect of temperature in thermo-mechanical computational models.

The present study focuses on having a better understanding of the buckling, post-buckling and failure characteristics of multilayered composite panels subjected to combined mechanical and thermal loads. Specifically, the objectives are

- to obtain the stability boundary of different types of laminates under axial compression and uniform temperature loading.

- to obtain the failure envelope of laminates in terms of the first-ply failure under combined thermal and axial loads.

- to study the effect of temperature sensitivity of mechanical and strength properties on the response and failure of laminates.

The study is performed using a finite element formulation based on the first-order shear deformation, von-Karman type non-linear plate theory. Most notably, temperature-dependent thermo-mechanical properties are also incorporated.

CHAPTER 2

FINITE ELEMENT FORMULATION AND FAILURE MODEL

2.1 Introduction

The aim of this chapter is to provide a geometrically nonlinear Mindlin type formulation for laminates. The finite element equations are derived based on the principle of minimum potential energy. The formulation is basically the one developed by Singh *et al.* (1996). It is based on Mindlin's plate theory (see, e.g., Hinton *et al*, 1975) which accounts for the through-the-thickness shearing effects, resulting in, plane sections normal to the midsurface remaining plane but not normal to the midsurface after deformation. This model has the advantage of requiring only C^0 continuity for all the primary variables, and hence, enables an easy formulation. Such a model readily accommodates moderately thick plates; however, they can exhibit locking when applied to thin plates. Extensive studies on Mindlin plate elements (Paugh *et al.*, 1978) envisage that the nine noded Lagrangian element, with selective integration of the shear terms, is quite adequate for predicting the response characteristics of both thin and thick plates.

2.2 Plate Deformation, Strains and Stress-Strain Relations

In the Mindlin Plate theory, the displacements $u=[u, v, w]^T$ at (x, y, z) are expressed as functions of the mid-plane ($z=0$) translations u_0, v_0 and w_0, and of the independent normal rotations θ_x and θ_y in the xz and yz planes, respectively:

$$u(x,y,z) = u_0(x,y) + z\theta_x(x,y) \tag{2.1}$$

$$v(x,y,z) = v_0(x,y) + z\theta_y(x,y) \tag{2.2}$$

$$w(x,y,z) = w_0(x,y) \tag{2.3}$$

For a Mindlin plate, the relevant Green's strain vector (Chia, 1980) is given as,

$$\{\varepsilon\} = \begin{bmatrix} \varepsilon_x \\ \varepsilon_y \\ \gamma_{xy} \\ \gamma_{xz} \\ \gamma_{yz} \end{bmatrix} = \begin{bmatrix} \frac{\partial u}{\partial x} + \frac{1}{2}\left(\frac{\partial u}{\partial x}\right)^2 + \frac{1}{2}\left(\frac{\partial v}{\partial x}\right)^2 + \frac{1}{2}\left(\frac{\partial w}{\partial x}\right)^2 \\ \frac{\partial v}{\partial y} + \frac{1}{2}\left(\frac{\partial u}{\partial y}\right)^2 + \frac{1}{2}\left(\frac{\partial v}{\partial y}\right)^2 + \frac{1}{2}\left(\frac{\partial w}{\partial y}\right)^2 \\ \frac{\partial u}{\partial y} + \frac{\partial v}{\partial x} + \frac{\partial u}{\partial x}\frac{\partial u}{\partial y} + \frac{\partial v}{\partial x}\frac{\partial v}{\partial y} + \frac{\partial w}{\partial x}\frac{\partial w}{\partial y} \\ \frac{\partial u}{\partial z} + \frac{\partial w}{\partial x} + \frac{\partial u}{\partial x}\frac{\partial u}{\partial z} + \frac{\partial v}{\partial x}\frac{\partial v}{\partial z} + \frac{\partial w}{\partial x}\frac{\partial w}{\partial z} \\ \frac{\partial v}{\partial z} + \frac{\partial w}{\partial y} + \frac{\partial u}{\partial y}\frac{\partial u}{\partial z} + \frac{\partial v}{\partial y}\frac{\partial v}{\partial z} + \frac{\partial w}{\partial y}\frac{\partial w}{\partial z} \end{bmatrix} \tag{2.4}$$

Introducing von Karman's assumptions (Fung, 1965) and noting that w is independent of z, eqn. (2.4) can be rewritten, using eqns. (2.1-2.3), as

$$\{\varepsilon\} = \{\varepsilon^0\} + z\{K\} \tag{2.5}$$

where

$$\{\varepsilon\} = [\varepsilon_x, \varepsilon_y, \gamma_{xy}, \gamma_{xz}, \gamma_{yz}]^T \tag{2.6}$$

$$\{\varepsilon^0\} = [\varepsilon_x^0, \varepsilon_y^0, \gamma_{xy}^0, \gamma_{xz}^0, \gamma_{yz}^0]^T \tag{2.7}$$

$$= \{\varepsilon_l^0\} + \{\varepsilon_{nl}^0\} \tag{2.8}$$

in which

$$\{\varepsilon_l^0\} = \left[\frac{\partial u_0}{\partial x}, \frac{\partial v_0}{\partial y}, \frac{\partial u_0}{\partial y} + \frac{\partial v_0}{\partial x}, \frac{\partial w_0}{\partial x} + \theta_x, \frac{\partial w_0}{\partial y} + \theta_y\right]^T \tag{2.9}$$

$$\{\varepsilon_{nl}^0\} = \left[\frac{1}{2}\left(\frac{\partial w_0}{\partial x}\right)^2, \frac{1}{2}\left(\frac{\partial w_0}{\partial y}\right)^2, \left(\frac{\partial w_0}{\partial x}\frac{\partial w_0}{\partial y}\right), 0, 0\right]^T \tag{2.10}$$

and

$$\{K\} = [K_x, K_y, K_{xy}, 0, 0]^T \tag{2.11}$$

$$= \left[\frac{\partial \theta_x}{\partial x}, \frac{\partial \theta_y}{\partial y}, \frac{\partial \theta_x}{\partial y} + \frac{\partial \theta_y}{\partial x}, 0, 0\right]^T \tag{2.12}$$

where the suffix '*l*' and '*nl*' stand for the linear and nonlinear parts, respectively, of the mid-plane strain components.

Based on the assumption that σ_z is negligible, the thermo-mechanical constitutive relations for the k^{th} lamina, oriented arbitrarily to the laminate axes, are given by,

$$\begin{bmatrix}\sigma_x\\ \sigma_y\\ \tau_{xy}\\ \tau_{yz}\\ \tau_{xz}\end{bmatrix}=\begin{bmatrix}Q_{11} & Q_{12} & Q_{13} & 0 & 0\\ & Q_{22} & Q_{23} & 0 & 0\\ & & Q_{33} & 0 & 0\\ & \text{Symmetric} & & k_1^2Q_{44} & k_1k_2Q_{45}\\ & & & & k_2^2Q_{55}\end{bmatrix}\begin{Bmatrix}\varepsilon_x-\alpha_x\Delta T\\ \varepsilon_y-\alpha_y\Delta T\\ \gamma_{xy}-2\alpha_{xy}\Delta T\\ \gamma_{yz}\\ \gamma_{xz}\end{Bmatrix} \tag{2.13}$$

where k_1, k_2 are the shear correction factors (Mindlin, 1951), Q_{ij} are the transformed reduced stiffness coefficients of a lamina (see Appendix I), $\alpha_x, \alpha_y, \alpha_{xy}$ are the transformed thermal expansion coefficients and ΔT is the temperature change.

2.3 Stress Resultants at the Mid-Plane of the Laminate

The stress resultants for a laminate with 'NL' number of layers as shown in fig.2.1 are given by

$$\{N\}=[N_x,N_y,N_{xy}]^T=\sum_{k=1}^{NL}\left[\int_{z_k}^{z_{k+1}}(\sigma_x,\sigma_y,\tau_{xy})dz\right]^T \tag{2.14}$$

$$\{M\}=[M_x,M_y,M_{xy}]^T=\sum_{k=1}^{NL}\left[\int_{z_k}^{z_{k+1}}(\sigma_x,\sigma_y,\tau_{xy})z\,dz\right] \tag{2.15}$$

$$\{Q\}=[Q_x,Q_y]^T=\sum_{k=1}^{NL}\left[\int_{z_k}^{z_{k+1}}(\tau_{xz},\tau_{yz})dz\right]^T \tag{2.16}$$

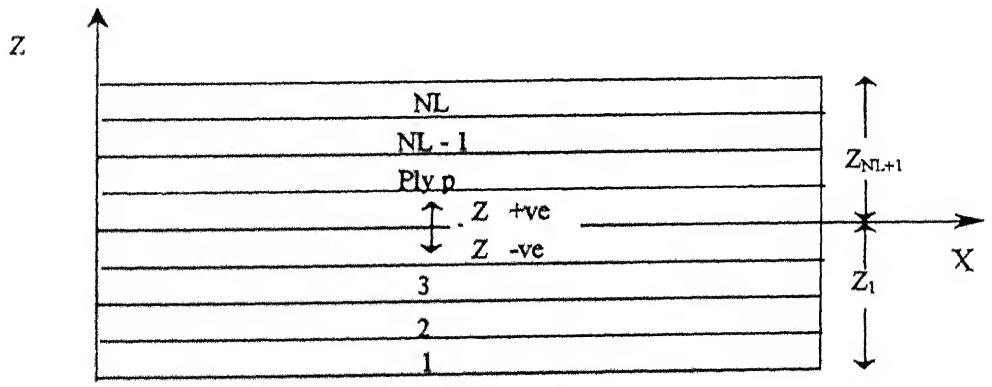

Fig. 2.1. Geometry of a NL layered laminate.

Substituting eqn. (2.5) in eqn. (2.13) and integrating through the thickness, the expression for stress resultants become

$$\begin{bmatrix} N_x \\ N_y \\ N_{xy} \\ M_x \\ M_y \\ M_{xy} \end{bmatrix} = \begin{bmatrix} [A] & : & [B] \\ \cdots & \cdots & \cdots \\ [B] & : & [D] \end{bmatrix} \begin{bmatrix} \varepsilon_x \\ \varepsilon_y \\ \gamma_{xy} \\ K_x \\ K_y \\ K_{xy} \end{bmatrix} - \begin{bmatrix} N_{tx} \\ N_{ty} \\ N_{txy} \\ M_{tx} \\ M_{ty} \\ M_{txy} \end{bmatrix} \tag{2.17}$$

$$\begin{bmatrix} N_x \\ N_y \\ N_{xy} \\ M_x \\ M_y \\ M_{xy} \end{bmatrix} = \begin{bmatrix} \overline{N}_x \\ \overline{N}_y \\ \overline{N}_{xy} \\ \overline{M}_x \\ \overline{M}_y \\ \overline{M}_{xy} \end{bmatrix} - \begin{bmatrix} N_{tx} \\ N_{ty} \\ N_{txy} \\ M_{tx} \\ M_{ty} \\ M_{txy} \end{bmatrix} \tag{2.18}$$

$$\begin{bmatrix} Q_x \\ Q_y \end{bmatrix} = \begin{bmatrix} E_{11} & E_{12} \\ E_{21} & E_{22} \end{bmatrix} \begin{bmatrix} \gamma_{xz} \\ \gamma_{yz} \end{bmatrix} \tag{2.19}$$

where $[A]$, $[B]$, and $[D]$ are 3X3 matrices with

$$A_{ij} = \sum_{k=1}^{NL} Q_{ij}(z_{k+1} - z_k) \quad \forall \; i,j \in [1,3] \tag{2.20}$$

$$B_{ij} = \frac{1}{2}\sum_{k=1}^{NL} Q_{ij}\left(z_{k+1}^2 - z_k^2\right) \quad \forall \; i,j \in [1,3] \tag{2.21}$$

$$D_{ij} = \frac{1}{3}\sum_{k=1}^{NL} Q_{ij}\left(z_{k+1}^3 - z_k^3\right) \quad \forall \; i,j \in [1,3] \tag{2.22}$$

$$E_{11} = k_2^2 \sum_{k=1}^{NL} Q_{55}(z_{k+1} - z_k) \tag{2.23}$$

$$E_{22} = k_1^2 \sum_{k=1}^{NL} Q_{44}(z_{k+1} - z_k) \tag{2.24}$$

$$E_{12} = E_{21} = k_1 k_2 \sum_{k=1}^{NL} Q_{45}(z_{k+1} - z_k) \tag{2.25}$$

$$\begin{bmatrix} N_{xx}, & M_{xx} \\ N_{yy}, & M_{yy} \\ N_{xxy}, & M_{xxy} \end{bmatrix} = [N_t, \quad M_t]$$

$$= \sum_{k=1}^{NL} \int_{z_k}^{z_{k+1}} \begin{bmatrix} Q_{11} & Q_{12} & Q_{13} \\ & Q_{22} & Q_{21} \\ sym & & Q_{31} \end{bmatrix} \begin{Bmatrix} \alpha_x \\ \alpha_y \\ 2\alpha_{xy} \end{Bmatrix} (1, \quad z)\, \Delta T\, dz \tag{2.26}$$

2.4 Total Lagrangian and Virtual Work Equation

The formulation is based on the virtual work equation for a continuum in the total Langrangian coordinate systems under assumptions of small strains and conservative loads. In the absence of body forces the virtual work equation can be written as,

$$\int_{V^0} \delta\varepsilon^T \sigma \, dV - \int_A \delta u^T p dA = 0 \tag{2.27}$$

where V^0 is the undeformed volume, σ is the Piola-Kirchoff stress vector and $\delta\varepsilon$ is variation of Green's strain vector due to variations of displacement u (δu) and p is the surface traction acting over an undeformed area A. Here δ denotes the first-variation. The variation of strain energy is given by,

$$\delta U = \int_{V^0} \delta\varepsilon^T \sigma dV^0 = \int_A \int_{-h/2}^{h/2} \left[\delta\varepsilon_x \sigma_x + \delta\varepsilon_y \sigma_y + \delta\gamma_{xy}\tau_{xy} + \delta\gamma_{yz}\tau_{yz} + \delta\gamma_{xz}\tau_{xz}\right] dz\, dA \tag{2.28}$$

Substituting the strain expressions of eqns. (2.5-2.8) and eqn. (2.11) in the eqn. (2.28) and using the stress resultant expression of eqns. (2.14-2.16), δU can be written as

$$\delta U = \int_A \left[\delta\varepsilon_x^0 N_x + \delta\varepsilon_y^0 N_y + \delta\gamma_{xy}^0 N_{xy} + \delta K_x M_x + \delta K_y M_y + \delta K_{xy} M_{xy} + \delta\gamma_{xz} Q_x + \delta\gamma_{yz} Q_y\right] dA \tag{2.29}$$

The external work done due to edge traction p_n and p_t which are the local normal and the tangential tractions, respectively, acting on edge (see fig. 2.2) and written in terms of the global edge tractions p_x and p_y, is given by

$$\delta V_t = -\int_S \int_{-h/2}^{h/2} \left(\delta u p_x + \delta v p_y\right) dz\, ds \tag{2.30}$$

The global edge traction p_x and p_y are given in terms of local edge traction p_n and p_t as,

$$\begin{Bmatrix} P_x \\ P_y \end{Bmatrix} = \begin{bmatrix} \cos\phi & -\sin\phi \\ \sin\phi & \cos\phi \end{bmatrix} \begin{Bmatrix} p_n \\ p_t \end{Bmatrix} \tag{2.31}$$

where ϕ is the orientation of local normal traction p_n with respect to global direction x (fig. 2.2). Substituting for u and v from eqns. (2.1-2.2) in the enq. (2.30) and carrying out

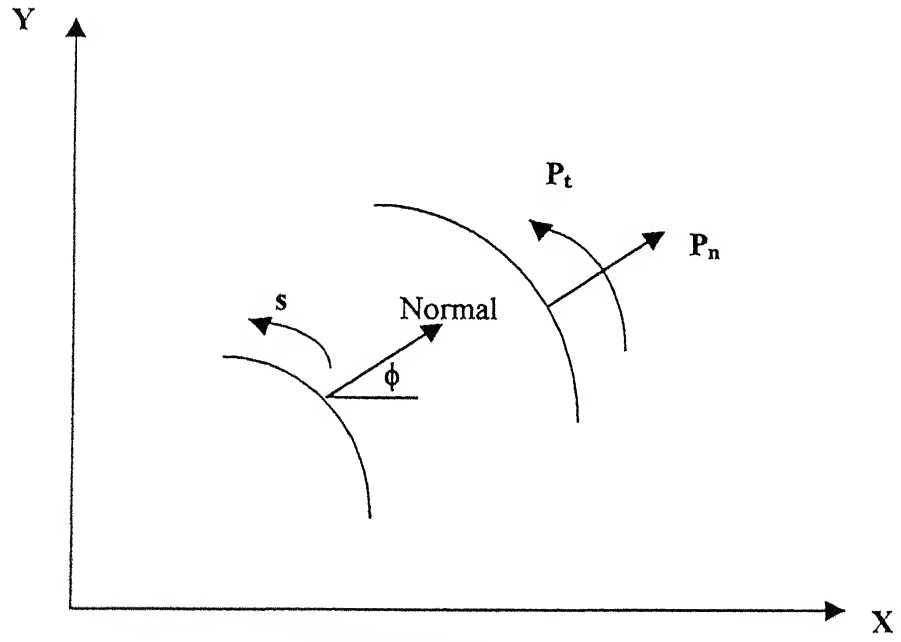

Fig 2.2 Edge Traction

the integration through the thickness, the variation of external potential energy due to in-plane forces becomes

$$\delta V_i = -\int_S \left(\delta u_0 P_x + \delta v_0 P_y\right) ds \tag{2.32}$$

where

$$\left[P_x, P_y\right]^T = \int_{-h/2}^{h/2} \left(p_x, p_y\right) dz \tag{2.33}$$

The variation of external potential energy with surface force is given by

$$\delta V_p = -\int_A \delta w_0 q \, dA \tag{2.34}$$

where q is the intensity of transverse loading. The variation of total potential energy, i.e., eqn. (2.27), can now be written in terms of the mid-plane forces and strain/displacement quantities as

$$\int_A \left(\delta\varepsilon_x^0 N_x + \delta\varepsilon_y^0 N_y + \delta\gamma_{xy}^0 N_{xy} + \delta K_x M_x + \delta K_y M_y + \delta K_{xy} M_{xy} + \delta\gamma_{xz} Q_x + \delta\gamma_{yz} Q_y\right) dA$$

$$- \int_S \left(\delta u_0 P_x + \delta v_0 P_y\right) ds - \int_A \delta w_0 q \, dA = 0 \tag{2.35}$$

2.5 Finite Element Formulation

The displacement within an element is expressed as a function of discrete nodal displacement:

$$\{u\}^e = [u, v, w, \theta_x, \theta_y]^T = \sum_{i=1}^{N} [N_i I_5]\{a_i\} \tag{2.36}$$

where

N = number of nodes in an element,

N_i, $\forall\ i \in [1, N]$ are the shape functions,

I_5 is 5 X 5 unit matrix,

$\{a_i\} = [u_{0i}, v_{0i}, w_{0i}, \theta_{xi}, \theta_{yi}]^T$ is the nodal displacement vector, the superscript 'e' refers to an element and the superscript 'T' indicates transpose of a matrix. The shape functions of a nine-noded Lagrangian element are given in Zienkiewicz (1992).

The virtual work equation (2.35) can be re-written as

$$\begin{aligned} \int_A \left[\delta\{\varepsilon_p^0\}^T\{N\} + \delta\{K\}^T\{M\} + \delta\{\varepsilon_s^0\}^T\{Q\}\right] dA \\ - \int_S \left(\delta u_0 P_x + \delta v_0 P_y\right) ds - \int_A \delta w_0 q\, dA = 0 \end{aligned} \tag{2.37}$$

$$\begin{aligned} \int_A \left[\delta\{\varepsilon_p^0\}^T\{\overline{N}\} + \delta\{K\}^T\{\overline{M}\} + \delta\{\varepsilon_s^0\}^T\{Q\}\right] dA \\ - \int_A \left[\delta\{\varepsilon_p^0\}^T\{N_l\} + \delta\{K\}^T\{M_l\}\right] dA \\ - \int_S \left(\delta u_0 P_x + \delta v_0 P_y\right) ds - \int_A \delta w_0 q\, dA = 0 \end{aligned} \tag{2.38}$$

where

$$\{\varepsilon_p^0\} = [\varepsilon_x, \varepsilon_y, \gamma_{xy}]^T \tag{2.39}$$

$$\{K\} = [K_x, K_y, K_{xy}]^T \tag{2.40}$$

$$\{\varepsilon_s^0\} = [\gamma_{xz}, \gamma_{yz}]^T \tag{2.41}$$

are, respectively, the in-plane, the bending and the transverse shear strain components of the total mid-plane strains of eqn. (2.7) and

$$\{N_l\} = [N_{lx}, N_{ly}, N_{lxy}]^T \tag{2.42}$$

$$\{M_l\} = [M_{lx}, M_{ly}, M_{lxy}]^T \tag{2.43}$$

2.5.1 First – variation of total in-plane strain

The in-plane strain vector $\{\varepsilon_p^0\}=[\varepsilon_x, \varepsilon_y, \gamma_{xy}]^T$ is expressed as a sum of linear and nonlinear components as given below:

$$\{\varepsilon_p^0\}=\{\varepsilon_p^0\}^l + \{\varepsilon_p^0\}^{nl} \tag{2.44}$$

where

$$\{\varepsilon_p^0\}^l = \begin{bmatrix} \frac{\partial}{\partial x} & 0 & 0 & 0 & 0 \\ 0 & \frac{\partial}{\partial y} & 0 & 0 & 0 \\ \frac{\partial}{\partial y} & \frac{\partial}{\partial x} & 0 & 0 & 0 \end{bmatrix} \begin{bmatrix} u_0 \\ v_0 \\ w_0 \\ \theta_x \\ \theta_y \end{bmatrix}^e \tag{2.45}$$

and

$$\{\varepsilon_p^0\}^{nl} = \frac{1}{2} \begin{bmatrix} \frac{\partial w_0}{\partial x} & 0 \\ 0 & \frac{\partial w_0}{\partial y} \\ \frac{\partial w_0}{\partial y} & \frac{\partial w_0}{\partial x} \end{bmatrix} \begin{bmatrix} 0 & 0 & \frac{\partial}{\partial x} & 0 & 0 \\ 0 & 0 & \frac{\partial}{\partial y} & 0 & 0 \end{bmatrix} \begin{bmatrix} u_0 \\ v_0 \\ w_0 \\ \theta_x \\ \theta_y \end{bmatrix} \tag{2.46}$$

Linear and nonlinear components of the in-plane strain can be written in terms of the elemental nodal displacement as,

$$\{\varepsilon_p^0\}^l = [B_{OL}]\{a\}^e \tag{2.47}$$

$$\{\varepsilon_p^0\}^{nl} = \frac{1}{2}[B_{ONL}]\{a\}^e \tag{2.48}$$

where

$$[B_{OL}] = [B_{OL,1}, B_{OL,2}, B_{OL,3}, ..., B_{OL,N}] \tag{2.49}$$

$$[B_{ONL}] = [B_{ONL,1}, B_{ONL,2}, B_{ONL,3}, ..., B_{ONL,N}] \tag{2.50}$$

Here, B_{OL} and B_{ONL} are the linear and the nonlinear strain-displacement matrices, respectively. The elemental nodal displacement vector is given as

$$\{a\}^e = [a_1, a_2, a_3, ..., a_n]^{eT} \tag{2.51}$$

where

$$\{a_i\} = [u_{0i}, v_{0i}, w_{0i}, \theta_{xi}, \theta_{yi}]^T \tag{2.52}$$

is the nodal displacement vector.

The component matrices of the elemental strain-displacement matrix are given as

$$[B_{OL,i}]=\begin{bmatrix} \frac{\partial N_i}{\partial x} & 0 & 0 & 0 & 0 \\ 0 & \frac{\partial N_i}{\partial y} & 0 & 0 & 0 \\ \frac{\partial N_i}{\partial y} & \frac{\partial N_i}{\partial x} & 0 & 0 & 0 \end{bmatrix} \tag{2.53}$$

$$[B_{ONL,i}]=[A_\theta][G] \tag{2.54}$$

where

$$[A_\theta]=\begin{bmatrix} \frac{\partial w_0}{\partial x} & 0 \\ 0 & \frac{\partial w_0}{\partial y} \\ \frac{\partial w_0}{\partial y} & \frac{\partial w_0}{\partial x} \end{bmatrix} \tag{2.55}$$

$$[G]=[G_1, G_2, G_3, ..., G_N] \tag{2.56}$$

The component matrices of G are

$$[G_i]=\begin{bmatrix} 0 & 0 & \frac{\partial N_i}{\partial x} & 0 & 0 \\ 0 & 0 & \frac{\partial N_i}{\partial y} & 0 & 0 \end{bmatrix} \tag{2.57}$$

The in-plane strain vector is now given in terms of A_θ and the Cartesian derivatives of shape functions as

$$\{\varepsilon_p^0\}=\left[B_{OL}+\frac{1}{2}A_\theta G\right]\{a\}^e \tag{2.58}$$

The first-variation of the total in-plane strain at the mid-surface is obtained by taking the first variation of eqn. (2.58):

$$\delta\{\varepsilon^0\}=[B_{OL}]\delta\{a\}^e+\frac{1}{2}\left[A_\theta G\delta\{a\}^e+\delta A_\theta G\{a\}^e\right] \tag{2.59}$$

Expressing w in terms of $[A_\theta]$ matrix as function of shape functions and re-arranging the first-variation of total in-plane strain can be expressed as

$$\delta\{\varepsilon_p^0\} = [[B_{OL}] + [A_\theta G]]\delta\{a\}^e \tag{2.60}$$

$$= [[B_{OL}] + [B_{ONL}]]\delta\{a\}^e \tag{2.61}$$

$$= [B_0]\delta\{a\}^e \tag{2.62}$$

2.5.2 First-variation of bending strain

The bending strain $\{K\} = [K_x, K_y, K_{xy}]^T$ can be expressed as

$$\{K\} = \begin{bmatrix} 0 & 0 & 0 & \frac{\partial}{\partial x} & 0 \\ 0 & 0 & 0 & 0 & \frac{\partial}{\partial y} \\ 0 & 0 & 0 & \frac{\partial}{\partial y} & \frac{\partial}{\partial x} \end{bmatrix} \begin{Bmatrix} u_0 \\ v_0 \\ w_0 \\ \theta_x \\ \theta_y \end{Bmatrix} \tag{2.63}$$

Substituting eqns. (2.1-2.3) in eqn. (2.63), the bending strain is expressed in terms of shape function as

$$\{K\} = [B_b]\{a\}^e \tag{2.64}$$

where

$\{a\}^e$ is the elemental nodal displacement vector as defined in eqn. (2.51). and

$$[B_b] = [B_{b,1}, B_{b,2}, B_{b,3}, \ldots, B_{b,N}] \tag{2.65}$$

in which the component matrices are

$$[B_{b,i}] = \begin{bmatrix} 0 & 0 & 0 & \frac{\partial N_i}{\partial x} & 0 \\ 0 & 0 & 0 & 0 & \frac{\partial N_i}{\partial y} \\ 0 & 0 & 0 & \frac{\partial N_i}{\partial y} & \frac{\partial N_i}{\partial x} \end{bmatrix} \tag{2.66}$$

The first-variation of the bending strain can now be expressed as

$$\delta\{K\} = [B_b]\delta\{a\}^e \tag{2.67}$$

2.5.3 First-variation of shear strain

The transverse shear strain, $\{\varepsilon_s^0\}=[\gamma_{xz},\gamma_{yz}]^T$

$$\{\varepsilon_s^0\}=\begin{bmatrix}0 & 0 & \dfrac{\partial}{\partial x} & 1 & 0\\ 0 & 0 & \dfrac{\partial}{\partial y} & 1 & 0\end{bmatrix}\begin{bmatrix}u_0\\ v_0\\ w_0\\ \theta_x\\ \theta_y\end{bmatrix} \tag{2.68}$$

can be expressed in terms of shape function as

$$\{\varepsilon_s^0\}=[B_s]\{a\}^e \tag{2.69}$$

where

$$[B_s]=[B_{s,1},B_{s,2},B_{s,3},\ldots,B_{s,N}] \tag{2.70}$$

in which the component matrices are

$$[B_{S,i}]=\begin{bmatrix}0 & 0 & \dfrac{\partial N_i}{\partial x} & N_i & 0\\ 0 & 0 & \dfrac{\partial N_i}{\partial y} & 0 & N_i\end{bmatrix} \tag{2.71}$$

The first-variation of shear strain is now expressed in terms of shape function as

$$\delta\{\varepsilon_s^0\}=[B_s]\delta\{a\}^e \tag{2.72}$$

2.5.4 Equivalent nodal load vector

The external virtual work due to in-plane loads and transverse forces in terms of shape function is expressed as

$$\delta v=\delta v_i+\delta v_p \tag{2.73}$$

$$\delta v=\delta\{a\}^{eT}\left[\int_A[B_N]^T\{P_s\}dA+\int_S[B_N]^T\{P_e\}ds\right] \tag{2.74}$$

where

$$\{P_s\}=[0\ \ 0\ \ q\ \ 0\ \ 0]^T \tag{2.75}$$

$$\{P_e\}=[P_x\ \ P_y\ \ 0\ \ 0\ \ 0]^T \tag{2.76}$$

$$[B_N]=[B_{N,1},B_{N,2},B_{N,3},\ldots,B_{N,N}] \tag{2.77}$$

in which the component matrices are

$$[B_{N,i}] = N_i [I_5] \tag{2.78}$$

where N_i is the shape function corresponding to the ith node and $[I_5]$ is a 5 X 5 unit matrix.

2.5.5 Nonlinear equilibrium equation

The total virtual work equation (2.35) is discretised for an element by substitution of eqns. (2.62), (2.67), (2.72) and (2.74);

$$\begin{aligned} \delta\{a\}^{eT} \int_A \left[[B_0]^T \{N\} + [B_b]^T \{M\} + [B_s]^T \{Q\} \right] dA \\ - \delta\{a\}^{eT} \left[\int_A [B_N]^T \{P_s\} dA + \int_S [B_N]^T \{P_e\} ds \right] = 0 \end{aligned} \tag{2.79}$$

from the equation. (2.18)

$$\begin{aligned} \delta\{a\}^{eT} \int_A \left[[B_0]^T \{\overline{N}\} + [B_b]^T \{\overline{M}\} + [B_s]^T \{Q\} \right] dA \\ - \delta\{a\}^{eT} \int_A \left[[B_0]^T \{N_t\} + [B_b]^T \{M_t\} \right] dA \\ - \delta\{a\}^{eT} \left[\int_A [B_N]^T \{P_s\} dA + \int_S [B_N]^T \{P_e\} ds \right] = 0 \end{aligned} \tag{2.80}$$

Since the nodal virtual displacement are arbitrary, the element nonlinear equilibrium equation becomes

$$\psi\{a\} = \int_A \left[[B_0]^T \{\overline{N}\} + [B_b]^T \{\overline{M}\} + [B_s]^T \{Q\} - [B_{ONL}]^T \{N_t\} \right] dA - R = 0 \tag{2.81}$$

where

$$R = \int_A \left[[B_{0L}]^T \{N_t\} + [B_b]^T \{M_t\} \right] dA + \int_A [B_N]^T \{P_s\} dA + \int_S [B_N]^T \{P_e\} ds \tag{2.82}$$

The eqn. (2.81) has a dual role of representing the total equilibrium equation; in an element form and in the assembled form.

2.6 Solution of Nonlinear Equilibrium Equation

The solution algorithm for the assembled nonlinear equations is based on the Newton-Raphson method. If an initial estimate of displacement vector gives the residual forces $\psi\{a\}_i \neq 0$, then an improved solution $\{a\}_{i+1}$ is obtained by equating to zero the linearized Taylor's series expansion of $\psi\{a\}_{i+1}$ in the neighbourhood of $\{a\}_i$ as

$$\psi\{a\}_{i+1} \cong \psi\{a\}_i + K_T \Delta\{a\}_i = 0 \tag{2.83}$$

where $\Delta\{a\}$ is the incremental displacement vector, and K_T is known as the tangent stiffness matrix evaluated at $\{a\}_i$ and is given by

$$K_T = \left[\frac{\partial \psi\{a\}_i}{\partial\{a\}}\right] \tag{2.84}$$

The linearized approximation to the relation between residual forces and incremental displacements at a point in the equilibrium path is given by eqn (2.83). The improved solution is then found as

$$\{a\}_{i+1} = \{a\}_i + \Delta\{a\}_i \tag{2.85}$$

The eqns. (2.83) and (2.84) represent the Newton-Raphson technique to the solution of nonlinear eqn. (2.81), which requires repeated calculation, and inversion of K_T matrix. To improve on the numerical stability and convergence of the solution, the load is applied in small increments. The iterative solution is checked for convergence using the following criteria.

$$\left[\frac{\psi^T \psi}{R^T R}\right]^{\frac{1}{2}} \times 100 \leq \beta \tag{2.86}$$

where β is sufficiently small number.

The tangent stiffness matrix K_T can be re-written as

$$K_T = \begin{bmatrix} \frac{\partial \psi_1}{\partial a_1} & \frac{\partial \psi_1}{\partial a_2} & \cdots & \frac{\partial \psi_1}{\partial a_m} \\ \cdots & \cdots & \cdots & \cdots \\ \cdots & \cdots & \cdots & \cdots \\ \frac{\partial \psi_m}{\partial a_1} & \frac{\partial \psi_m}{\partial a_2} & \cdots & \frac{\partial \psi_m}{\partial a_m} \end{bmatrix} \tag{2.87}$$

in which the subscript 'm' refers to the total degree of freedom per element. Differentiating ψ_i with respect to a_j and noting that $\frac{\partial R_i}{\partial a_j} = 0$ for conservative loads, the tangent stiffness matrix assumes the following form (see Appendix II).

$$K_T = \int_A \left[\begin{bmatrix} B_0^T & B_b^T & B_s^T \end{bmatrix} \begin{bmatrix} [A] & [B] & [0] \\ [B] & [D] & [0] \\ [0] & [0] & [E] \end{bmatrix} \begin{bmatrix} B_0 \\ B_b \\ B_s \end{bmatrix} + [G]^T \begin{bmatrix} N_x & N_{xy} \\ N_{xy} & N_y \end{bmatrix} [G] \right] dA \qquad (2.88)$$

Substituting for the matrices B_0, B_b, B_s and G in the preceding equation one obtains

$$K_T = K_L + K_{NI} + K_\sigma \qquad (2.89)$$

where the constant linear stiffness matrix K_L is

$$\begin{aligned} K_L = \int_A \left[[B_{OL}]^T [A][B_{OL}] + [B_b]^T [B][B_{OL}] \right] dA \\ + \int_A \left[[B_{OL}]^T [B][B_b] + [B_b]^T [D][B_b] + [B_s]^T [E][B_s] \right] dA \end{aligned} \qquad (2.90)$$

the initial displacement matrix K_{NL} is

$$\begin{aligned} K_{NL} = \int_A \left[[B_{OL}]^T [A][B_{ONL}] + [B_{ONI}]^T [A][B_{OL}] + [B_{ONI}]^T [A][B_{ONL}] \right] dA \\ + \int_A \left[[B_b]^T [B][B_{ONL}] + [B_{ONI}]^T [B][B_b] \right] dA \end{aligned} \qquad (2.91)$$

and the initial stress matrix K_σ is

$$K_\sigma = \int_A [G]^T \begin{bmatrix} N_x & N_{xy} \\ N_{xy} & N_y \end{bmatrix} [G] dA \qquad (2.92)$$

The integration of expression for $\Psi\{a\}$ and K_T is carried out using the Gaussian quadrature. A selective integration scheme is adopted with 3 X 3 integration rule to evaluate integrals of the functions of the membrane and the bending behavior and a 2 X 2 integration rule is used for the transverse shear component. Predominance of zeroes in matrices B_0, B_b, B_s, and G indicates that the expression for $\Psi\{a\}$ and K_T are best calculated explicitly, giving only the non-zero values

2.7 Failure Criteria

A detailed review of various failure criteria has been made by Reddy&Pandey (1987) and Reddy & Reddy (1992). Herein, for predicting the laminate failure, the first-ply failure analysis is done based on the Tsai-Wu criterion (1971); it is postulated that a failure surface in stress space exists in the form

$$F_i\sigma_i + F_{ij}\sigma_i\sigma_j = 1 \qquad i, j = 1,\ldots,6 \qquad (2.93)$$

wherein F_i and F_j are strength tensors of the second and fourth rank, respectively, and the usual contracted stress notation is used except that $\sigma_4 = \tau_{23}$, $\sigma_5 = \tau_{31}$, and $\sigma_6 = \tau_{12}$ (in the principal material direction). The tensor polynomial form of the Tsai-Wu criterion is given below :

$$F_1\sigma_1 + F_2\sigma_2 + F_3\sigma_3 + 2F_{12}\sigma_1\sigma_2 + 2F_{13}\sigma_1\sigma_3 + 2F_{23}\sigma_2\sigma_3 + F_{11}\sigma_1^2 + F_{22}\sigma_2^2 + F_{33}\sigma_3^2 + F_{44}\sigma_4^2 + F_{55}\sigma_5^2 + F_{66}\sigma_6^2 \geq 1 \qquad (2.94)$$

where

$$F_1 = \frac{1}{X_t} - \frac{1}{X_c}; \quad F_2 = \frac{1}{Y_t} - \frac{1}{Y_c}; \quad F_3 = \frac{1}{Z_t} - \frac{1}{Z_c};$$

$$F_{11} = \frac{1}{X_t X_c}; \quad F_{22} = \frac{1}{Y_t Y_c}; \quad F_{33} = \frac{1}{Z_t Z_c};$$

$$F_{44} = \frac{1}{R^2}; \; F_{55} = \frac{1}{S^2}; \; F_{66} = \frac{1}{T^{12}};$$

$$F_{12} = -\frac{1}{2}\left(\frac{1}{\sqrt{X_t X_c Y_t Y_c}}\right)$$

$$F_{13} = -\frac{1}{2}\left(\frac{1}{\sqrt{X_t X_c Z_t Z_c}}\right)$$

$$F_{23} = -\frac{1}{2}\left(\frac{1}{\sqrt{Y_t Y_c Z_t Z_c}}\right)$$

And all other strength tensor components are zero.

For the composite laminates under plane stress conditions, lamina failure is said to have occurred when the state of stress at any point with in the lamina (at mid-thickness) satisfies the tensor polynomial form of the Tsai-Wu criterion in which terms associated with normal stress component in third principal material directions are omitted. Equation (2.94) becomes

$$F_1\sigma_1 + F_2\sigma_2 + 2F_{12}\sigma_1\sigma_2 + F_{11}\sigma_1^2 + F_{22}\sigma_2^2 + F_{44}\sigma_4^2 + F_{55}\sigma_5^2 + F_{66}\sigma_6^2 \geq 1 \qquad (2.95)$$

The nodal point stresses are calculated using the finite element model and the stresses are checked for the above failure condition. The failure of a node in the lamina represents the failure of that particular layer. The first-ply failure load refers to the first instant at which one, or more than one ply fails at the same load.

CHAPTER 3

NUMERICAL RESULTS AND DISCUSSION

In this chapter, numerical illustrations are given for symmetrically laminated plates subjected to combined thermal and compressive edge loading. The finite element formulation presented in the previous chapter is used to study the response, mainly in terms of the stability and the first-ply failure envelopes. Regarding the prediction of the first-ply failure, the Tsai-Wu failure criterion is incorporated in the computational model. Numerical studies deal with the cases of perfectly bonded symmetric Graphite/Epoxy laminates having temperature dependent/independent, mechanical properties.

3.1 Convergence and Validation Study

The capability of the finite element formulation in predicting the post-buckling response under thermal loads is demonstrated by comparing results with those obtained by Huang and Tauchert (1991). An infinite layered regular anti-symmetric angle-ply laminate, with temperature independent material properties and subjected to uniform temperature rise, is considered. The plate is square, simply supported with edges restrained against the inplane normal displacement and free to move in the tangential direction. Figure 3.1 gives temperature versus central deflection curves as obtained by using successive refined meshes. It is observed that results of 5X5 and 6X6 meshes are in good agreement with those of Huang and Tauchert (1991). To save computing time without sacrificing accuracy, the 5X5 mesh is adopted in the entire analysis. In addition, the computer program has checked well with the results given by Chen and Chen (1989) and Noor *et al.* (1993) for the thermal post-buckling response under different boundary conditions, laminate sequences and material properties. It may be mentioned here that the validation

study for the stresses under inplane mechanical loads has been reported by Singh et al. (1997).

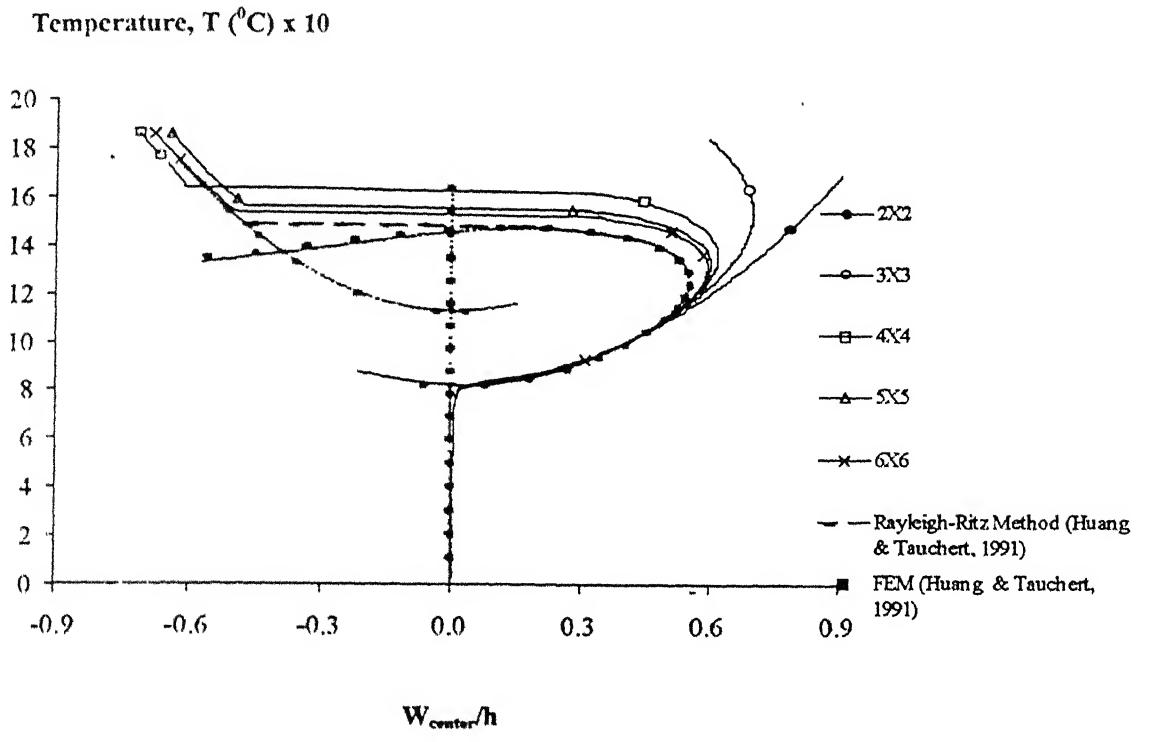

(E_L =130.3 GPa, E_T =9.37 GPa, G_{LT} =4.502 GPa, G_{TT} =1.724 GPa, ν_{LT} =0.33, α_L =0.139x10^{-6}, α_T =9x10^{-6}, $L_1 = L_2$ =0.254m, b/h = 125, θ=30^0)

Fig. 3.1 Convergence and validation of solution

The program is also checked for the case of combined thermal and mechanical loads by comparing the results of the buckling strength obtained by Noor and Peters (1992) for $(+45/-45/0/90)_{2s}$ and $(+30/-30)_{4s}$ laminates. The laminates are simply supported, with edges free to move in the normal direction but restrained in the tangential direction, and subjected to a compressive load and a uniform temperature rise. As can be seen from fig. 3.2, the results match quite well.

3.2 Analysis Details

In the present study, five types of graphite/epoxy composites are considered; the lamination scheme is given in Table 3.1. It is assumed that the laminate has perfectly

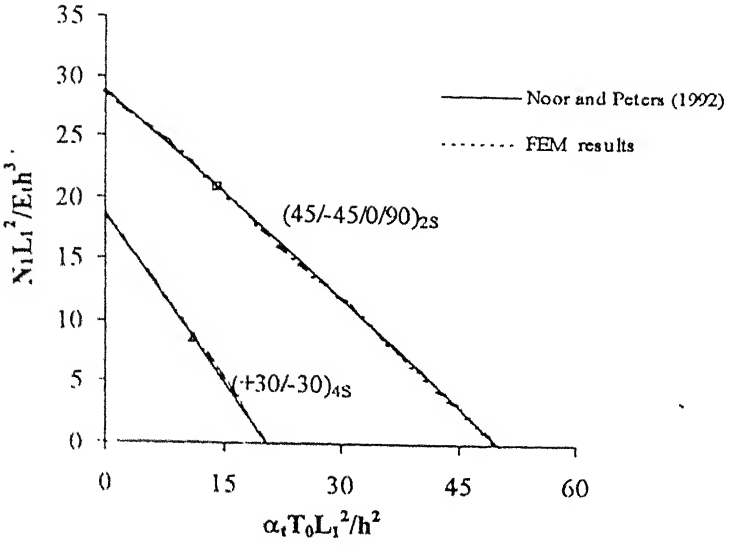

(E_L=130.3 GPa, E_T=9.37 GPa, G_{LT} =4.502 GPa, G_{TT} =1.724 GPa, ν_{LT} = 0.33, α_L= 0.139x10^{-6}, α_T =9x10^{-6}, L_1 = L_2 =0.254m, b/h = 125)

Fig. 3.2 Verification of solution under combined loading

bonded layers and during loading no delamination occurs. The panels are subjected to a combined action of the axial compressive load, N_x and the uniform temperature rise, T.

Table 3.1 Composite panels considered

Lamination scheme	$(\pm 45/0/90)_{2s}$	$(\pm 45/0_2)_{2s}$	$(\pm 45/0_6)_s$	$(\pm 45)_{4s}$	$(0/90)_{4s}$

The geometric properties and boundary conditions are given in fig. 3.3; these are the same as adopted by Noor and Peters (1992). The boundary conditions correspond to a simply supported laminate, with normal displacements permitted and shear displacements restrained on all edges. It may be noted that at corner points all the five degrees of freedom are restrained. The material properties of the laminates are taken as in Chen *et al.* (1985). Therein, temperature-dependent mechanical properties are derived analytically based on the rule of mixtures in conjunction with a glass transition temperature of 200°C for epoxy. In addition, the graphite fiber is assumed to retain its stiffness upto 3300°C. The elastic moduli and thermal expansion coefficients are listed in

Table 3.2, in which E, G and μ represent the Young's modulus, the shear modulus and the Poisson's ratio, while α denotes the coefficient of thermal expansion.

Geometric parameters

L_1 = 254 mm
L_2 = 254 mm
Thickness of individual layers=0.127 mm

Boundary conditions

At $x = 0, a$:
$v = w = \theta_y = 0$

At $y = 0, b$
$u = w = \theta_x = 0$

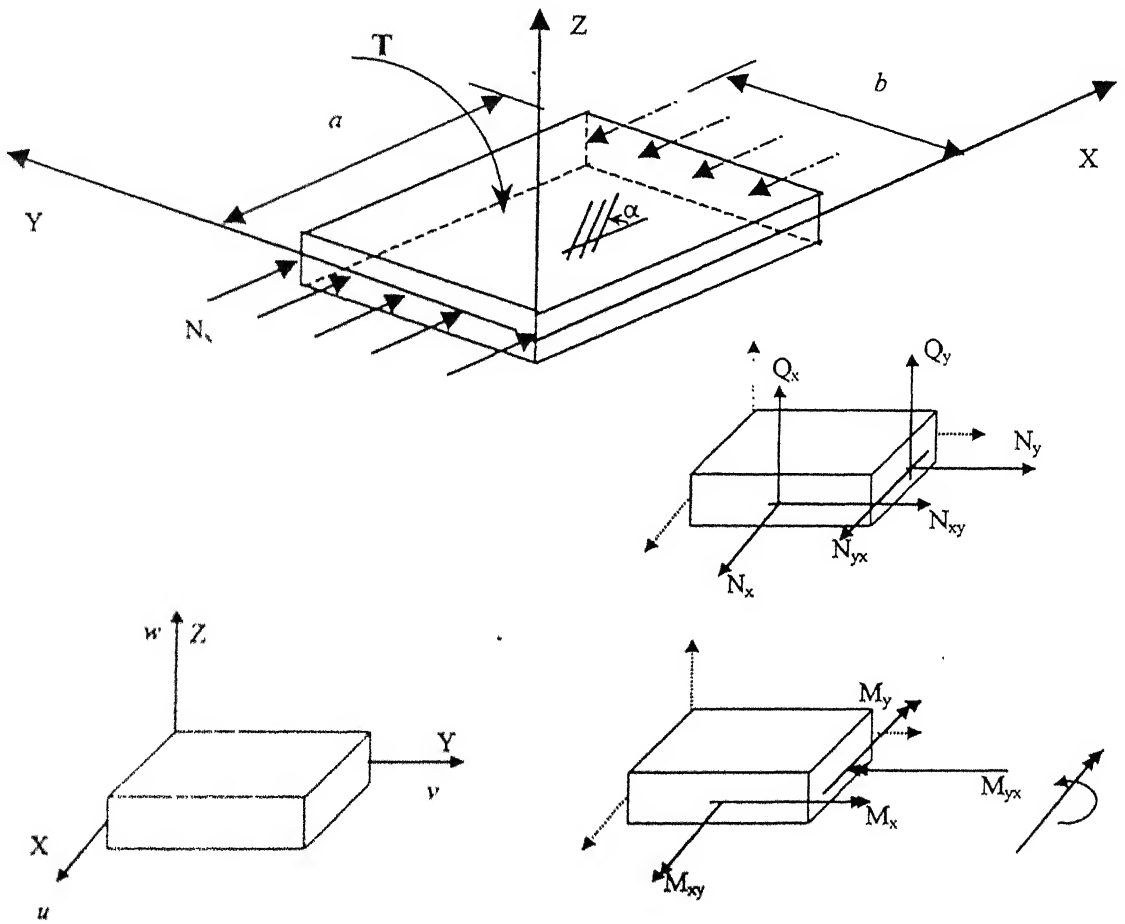

Fig. 3.3 Details of geometry, boundary conditions and sign conventions for stress resultants and generalized displacements.

Regarding the strength, for temperature exceeding 200°C, it is assumed that Gr/Ep strength decreases linearly to zero at a temperature when epoxy has been completely

cooked out. The net effect of the epoxy cooked out is to deplete the ability for the load transfer from one fiber strand to another. Based on the limited number of experiments on Gr/Ep at high temperature, the temperature-dependent strength properties of a single ply Gr/Ep composite were developed, and are tabulated in Table 3.3. (Chen et al 1985). Mechanical and the strength properties are assumed to have a linear variation for intermediate temperatures. In the analysis, the initial body temperature of the plate is taken as 20°C. It implies that at this temperature the laminate is stress free.

Table 3.2: Material mechanical properties

$(G_{12} = G_{13} = G_{23})$

Properties	Temperature (C°)				
	20	200	260	600	3316
E_1 (GPa)	141	141	141	141	141
E_2 (GPa)	13.1	10.3	0.138	0.0069	0.0069
G_{12} (GPa)	9.31	7.45	0.069	0.0034	0.0034
$\nu_{12} = \nu_{21}$	0.28	0.28	0.28	0.28	0.28
ν_{23}	0.49	0.49	0.49	0.49	0.49
α_1 (10^{-6}/ deg C)	0.018	0.054	0.054	0 054	0.054
α_2 (10^{-6}/ deg C)	21.6	37.8	37.8	37.8	37 8

Table 3.3: Material strength properties

$(X_t = X_c, S = R' = T')$

Temperature (°C)	Strength			
	X_t (MPa)	Y_t (MPa)	Y_c (MPa)	S (MPa)
20	1650	58.9	236	106
200	1650	46.5	186	84
260	↓	0.0	0.0	0.0
740	330			
3316	330			

As mentioned earlier, numerical results are obtained by using a 5X5 discretisation for the full laminate. The details of the finite element mesh and locations of Gauss points with in the elements are shown in fig. 3.4. Although results are obtained for all five lamination

schemes given in Table 3.1, the detailed investigation, whenever required, is carried out for the quasi-isotropic laminate only.

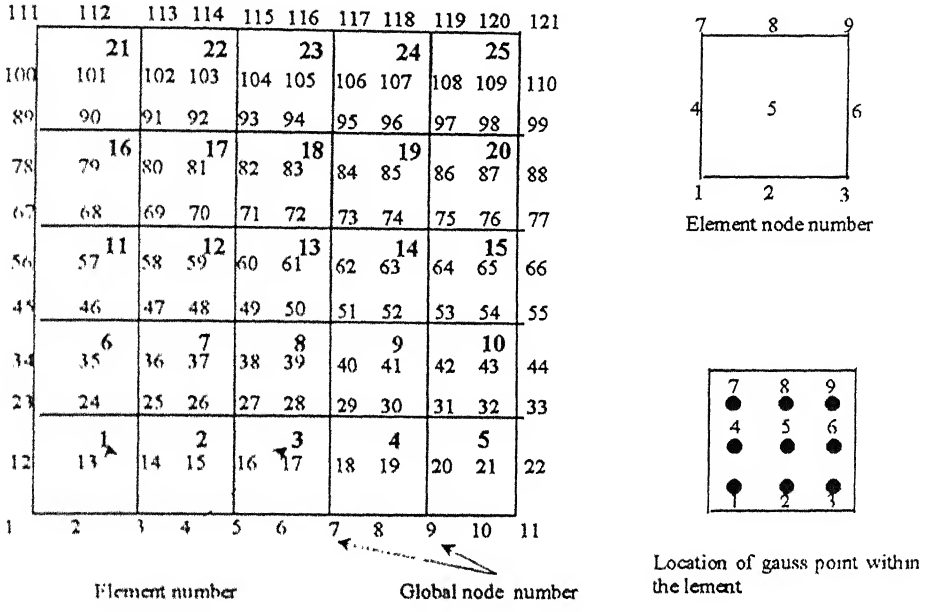

Fig. 3.4 Element and node numbering scheme for the laminated plate

3.3 Numerical Studies

3.3.1 Thermal post-buckling response

The thermal post-buckling response of 16-layered quasi-isotropic panels under uniform temperature loading is shown in fig. 3.5. There is a remarkable variation in the response and failure temperature for thermal dependent and independent material properties. In the process of temperature rise, temperature dependent properties reduce the stiffness of the laminate, thus causing variations in pre and post buckling deformations, critical temperature etc.

For Graphite/Epoxy composites, the response reveals a snap-through type behavior on the application of temperature beyond 200°C. This tends to decrease the deformation after 200°C and the first-ply failure occurs at 259.5°C. This peculiar variation is due to

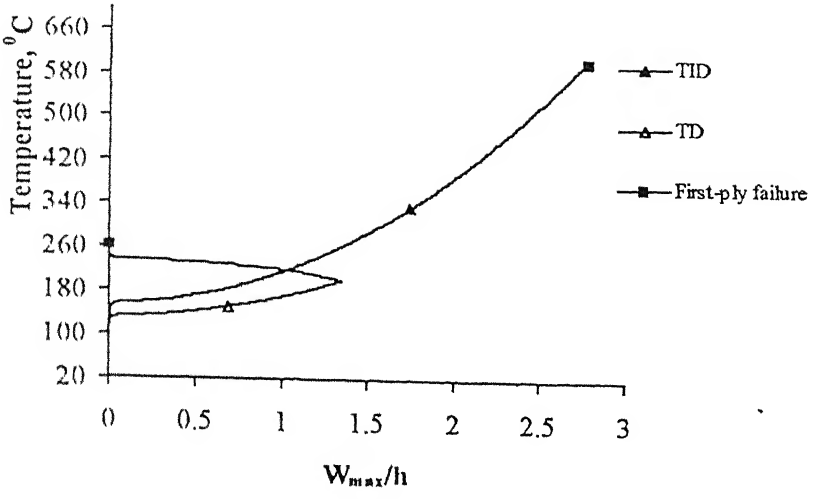

Fig. 3.5 Response of $(\pm 45/0/90)_{2s}$ laminate considering thermal dependent (TD) and independent (TID) material properties

sudden decrease in mechanical properties occurring after the glass transition temperature of epoxy at 200°C. From the figure, it is clear that first-ply failure temperature is well above the glass transition temperature. Therefore, the response after glass transition temperature is insignificant and it can be considered that the attainment of glass transition temperature is the failure of the composite. From the literature review, it is noticed that there are only few studies which have considered the temperature dependency in predicting the responses at elevated temperature. In the subsequent analysis, responses with temperature-dependent material properties are restricted to a maximum temperature of 200°C. It may be mentioned here that similar response characteristics are observed in remaining four laminates listed in Table 3.1.

3.3.2 Stability envelope

There could be various combinations of applied temperature and the axial compression at which the instability (buckling) may occur. The totality of such critical (bifurcation) points in the axial load-temperature space constitutes the stability boundary that separates regions of stability and instability. The stability boundary defines an implicit relationship (or an interaction) between the two parameters; the axial compression and the temperature, which, for a $(45/-45/0/90)_{2s}$ laminate is shown in fig. 3.6. In the interaction curve, the axial load N_x is nondimensionalised as $N_x b^2/E_2 h^3$ As can be seen from the

figure, with an increases in temperature the load required to cause buckling goes on decreasing. It is so because the total axial compressive load gets enhanced due to the boundary constraints. The response when temperature-independent material properties are considered, is very similar to those reported by Noor & Peters (1992) and Argyris & Tenek (1995). When thermal dependency is accounted for, the stability boundary moves inward as the temperature increases, implying that at a given temperature it requires lesser load to cause buckling as compared to the thermally independent case. From the figure it is clear that the variation in response (with and without thermal-dependent properties) is more pronounced at higher temperatures.

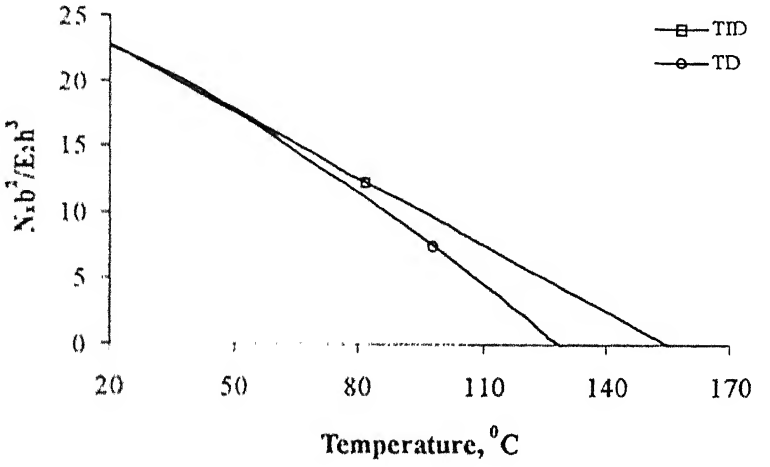

Fig. 3.6 Stability envelope for $(\pm 45/0/90)_{2s}$ laminate considering thermal dependent (TD) and independent (TID) material properties

The stability boundaries for all panels listed in Table 3.1 are displayed in one single figure 3.7. Although the nature of stability interaction curves is similar in all cases, the buckling strength under independent loads (i.e. either compression or temperature) is significantly different for different laminates. For example, under the axial load the buckling strength is the least for a cross-ply laminate, i.e. $(0/90)_{4s}$, and the maximum for a $(\pm 45/0)_6$ laminate; but the trend changes when only thermal loads are considered. One interesting observation is that all interaction curves can, more or less, be approximated by straight lines and hence can be represented by a simple equation.

3.3.2 First-ply failure envelope

The first-ply failure interaction for a quasi-isotropic laminate, i.e. $(45/-45/0/90)_{2s}$, under combined thermal and inplane compressive loads is shown in fig. 3.8. Such a graph gives

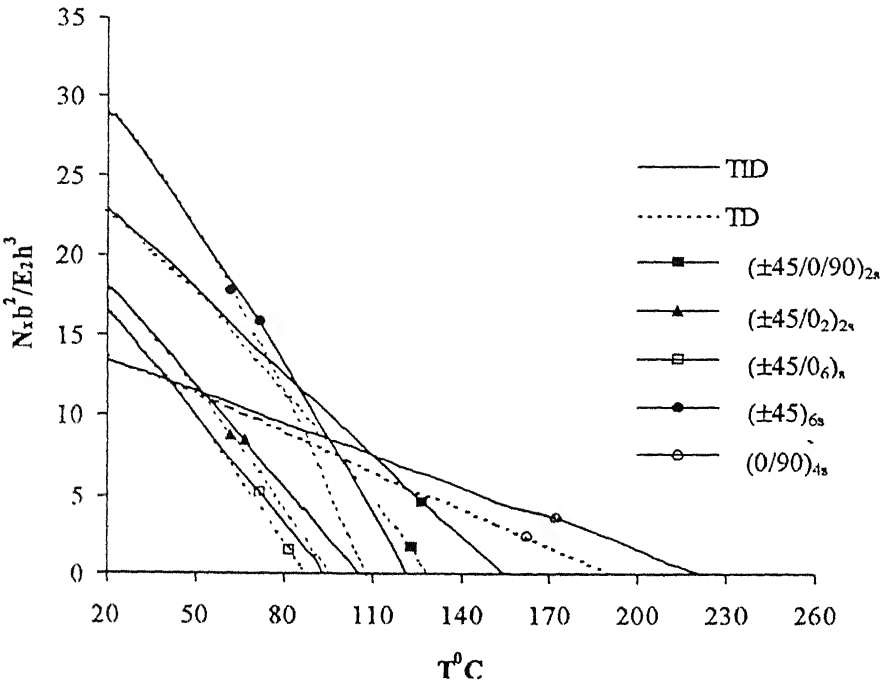

Fig. 3.7 Stability envelopes considering thermal dependent (TD) and independent (TID) material properties

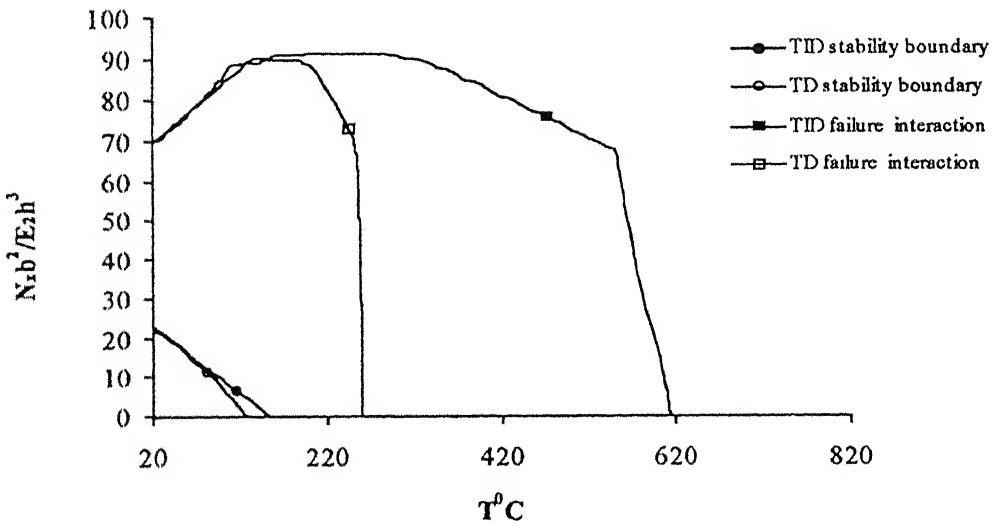

Fig. 3.8 Stability and failure envelopes for $(+45/-45/0/90)_{2s}$ laminate considering thermal dependent (TD) and independent (TID) material properties

information regarding the maximum compressive load that can be applied at a given temperature from the consideration of the first-ply failure. The interaction curve shows a +ve slope as temperature increases beyond 20^0C but it changes at elevated temperatures. As is obvious, with temperature rise, the plate can withstand more load than at 20^0C

(zero thermal load). However, at elevated temperatures, the curve is associated with a high negative gradient, which implies that the capacity to withstand the axial compressive load decreases rapidly. Interestingly, the nature of the first-ply failure envelope is distinctly different from that of the stability envelope. In fig. 3.8, the inclusion of thermal dependent material properties imparts considerable changes in the failure predictions under the combined loading. The graph shows that the plate can withstand hardly any loads, beyond 200^0C.

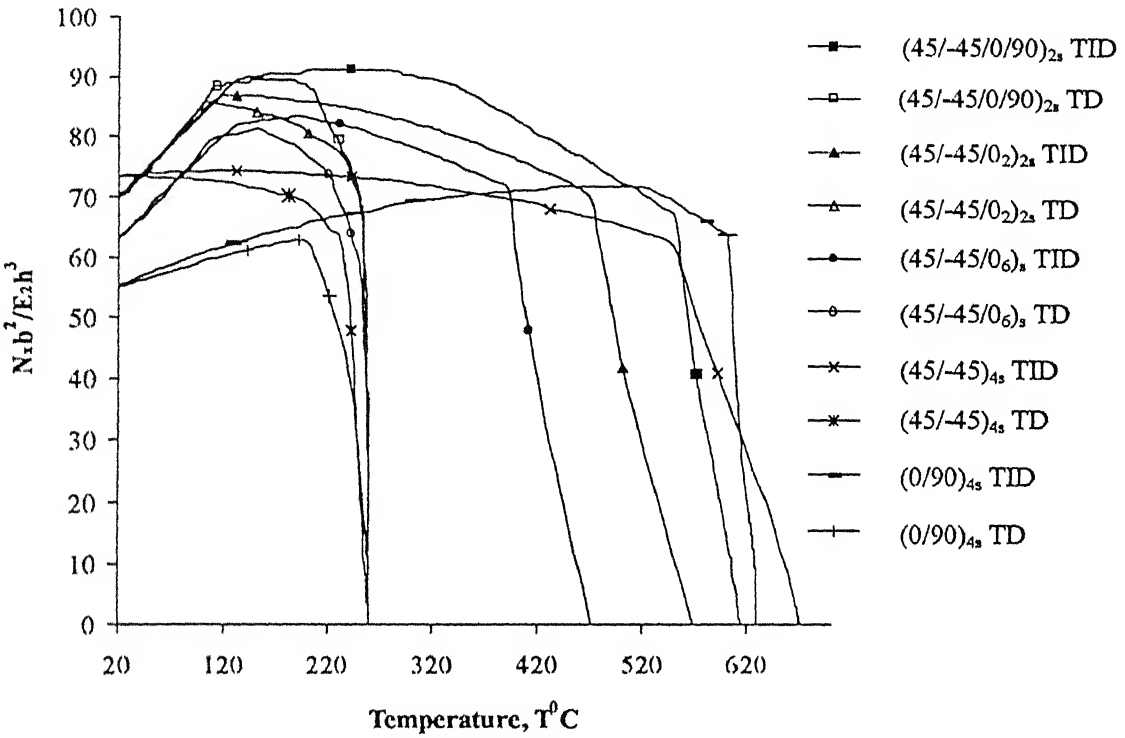

Fig. 3.9 First-ply failure envelopes considering thermal dependent (TD) and independent (TID) material properties

Figure 3.9 gives failure envelopes for all laminates listed in Table 3.1, with and without considering thermal dependent material properties. As can be seen, the peculiar nature of the failure interaction curve (as compared to the stability interaction curves) exists for all five laminates considered. The interaction curve for the cross-ply laminate, i.e. $(0/90)_{4s}$, gives a lower bound while that for the quasi-isotropic laminate, i.e. $(+45/-45/0/90)_{2s}$, yields an upper bound to first-ply failure envelopes.

In order to gain a better understanding of the peculiar nature of first-ply failure envelopes, it is necessary to gain an insight into the deformation response and the associated stress-distribution the resultant of which causes the failure. In this regard, a detailed study is made for the quasi-isotropic laminate, i.e. $(45/-45/0/90)_{2s}$, with temperature independent material properties.

Deformation responses in terms of maximum transverse displacement and edge displacement are displayed in fig. 3.10 and fig. 3.11, respectively. The transverse deflection under temperature rise is already given in fig. 3.5 and it is noticed that buckling occurs at 155^0C. Figure 3.10 shows the axial load versus the maximum deflection variation for a given temperature rise upto the first ply failure. At the room temperature ($T=20^0$C) the buckling occurs for a non-dimensionalised value of the axial compression equal to 23.5. In addition, the temperature rise is associated with an increased transverse deflection and the graph shows that the deflection increases under further application of compressive loads for all temperature ranges.

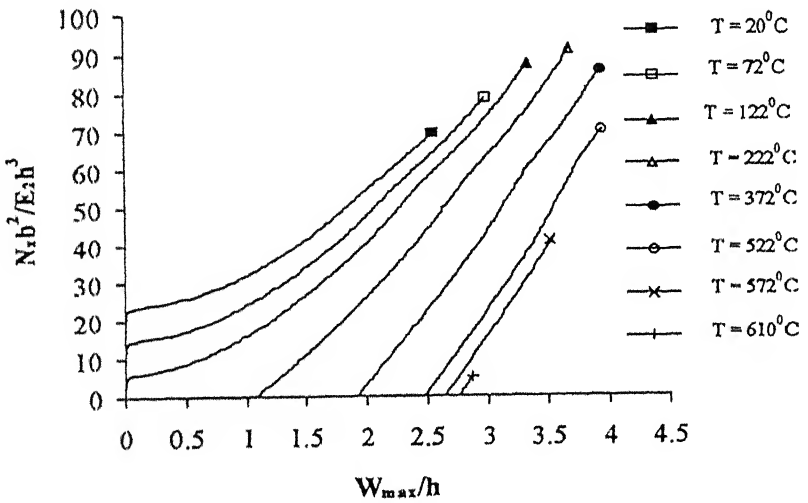

Fig.3.10 Transverse deflection for $(45/-45/0/90)_{2s}$ under combined loading at different temperature interval

The inplane displacement is calculated at the center of the edge, x=0 (node 56 in fig. 3.4). Figures 3.11a & b show the variation of the edge displacement under the axial

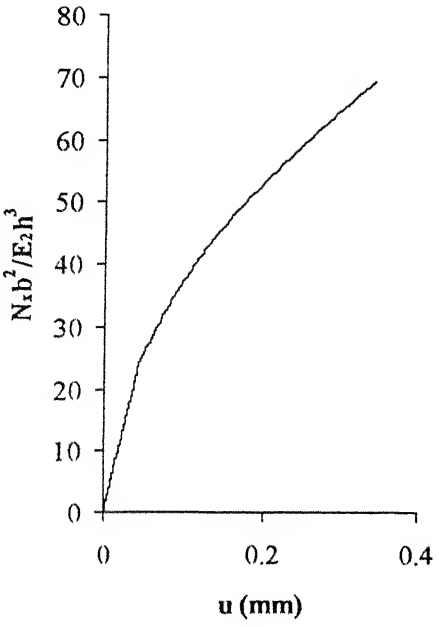

Fig. 3.11a Edge displacement under axial compression at x = 0, node 56

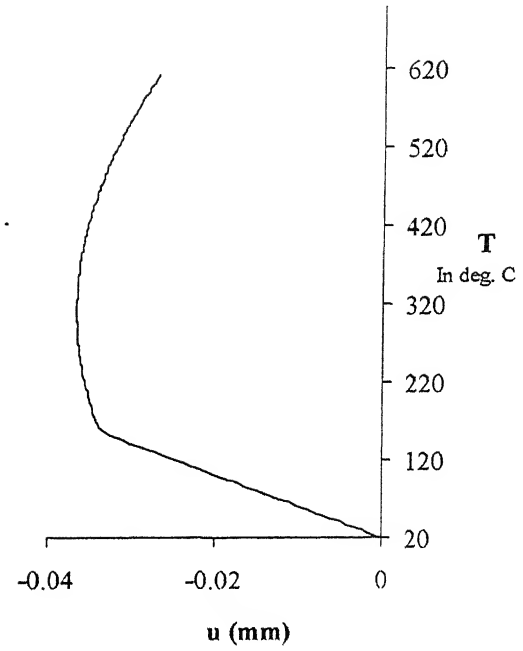

Fig. 3.11b Edge displacement under temperature rise at x = 0, node 56

compression and the uniform temperature rise, respectively. From fig. 3.11a it is clear that with an increase of compressive load, the edge moves in the +ve x-direction. On the other hand, under the temperature rise, the plate exhibits expansion (fig. 3.11b), but beyond the buckling temperature, the expansion becomes less prominent followed by an inward movement of the edge. Thus, in the pre -buckling range, edge displacements (at x=0, a; node=56, 66) under the temperature rise and the axial compression are opposite in nature, while in the post-buckling range (near failure) the plate deforms in similar ways (edge shortening). It may be noted that edges at y=0, b undergo expansion when subjected to the compressive load (in the x-direction) and temperature rise.

The pattern of the distribution of stresses in the laminate (at the failure location) is of paramount importance in the understanding of failure characteristics. For initial temperature ranges at which the failure interaction curve shows a higher positive gradient (see fig3.8), the failure is noticed in the second layer from the bottom (lamina orientation, $\alpha = -45^0$) at nodes 1 and 121 (diagonally opposite corners). For higher temperature ranges, the failure is observed in the 15^{th} layer ($\alpha = -45^0$; nodes =1, 121). The mode of failure in both the case is of transverse type. The stress values are obtained

at these lamina failure locations. Graphs are plotted between the non-dimensionalised axial load and stresses (in GPa) for different initial temperature rise. First, the stress distributions at the failure location associated with initial values of temperature under combined loading (at node, 1 layer, 2) are cosidered. At this particular location, it is observed that the stress σ_y has the same values as σ_x, while other stress components (except τ_{xy}) are close to zero. Figures 3.12a & b give the variation of σ_x and τ_{xy}, while fig. 3.12c shows the distribution of stresses σ_x and τ_{xy} under the uniform temperature rise. Whereas at $T=20^0C$, the plate developes compressive stresses under the axial compression (fig. 3.12a) the stress σ_x is tensile under the temperature rise (fig. 3.12c). Thus, at this particular node, the stress σ_x under two loads is opposite in nature. The same holds for the shear stress τ_{xy} as well. Thus, the laminate when subjected to a temperaute higher than 20^0C, is required to be subjected to an increased axial load (compressive) for the attainment of first-ply failure conditions. This results in a positive gradient in the failure envelope (see fig. 3.8).

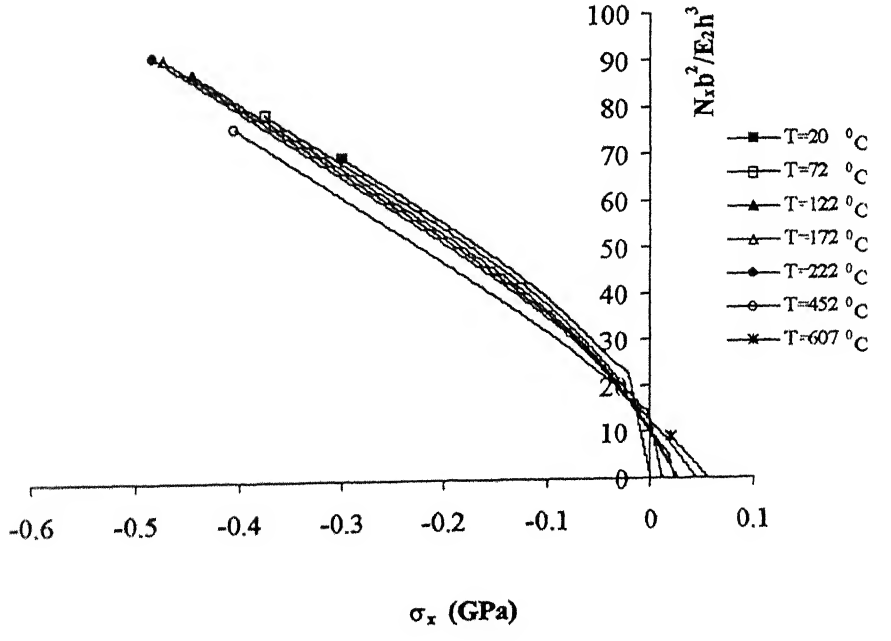

Fig. 3.12a Variation of stress σ_x at node 1, layer 2

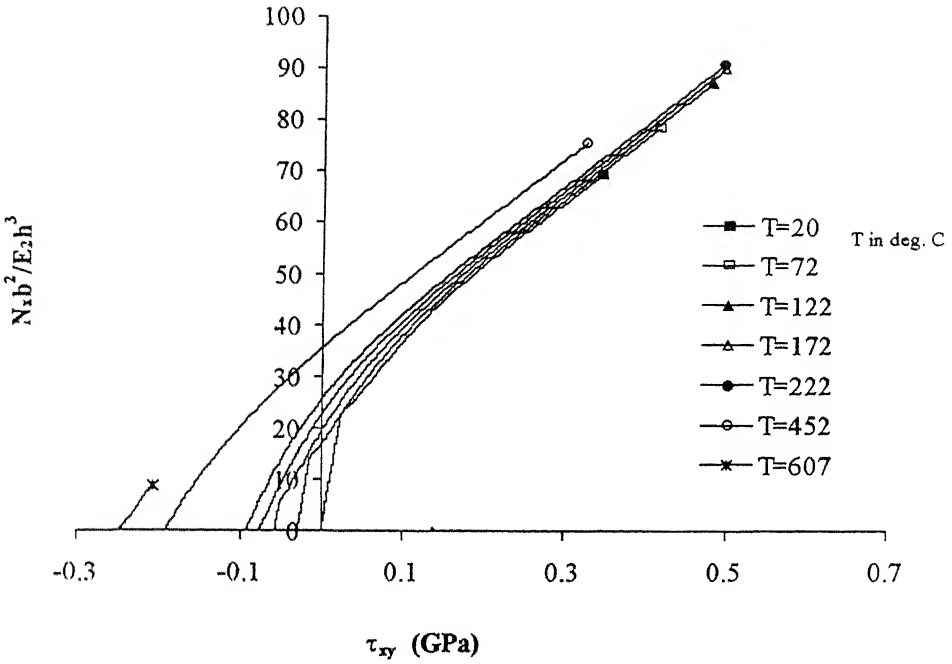

Fig. 3.12b Variation of stress τ_{xy} at node 1, layer 2

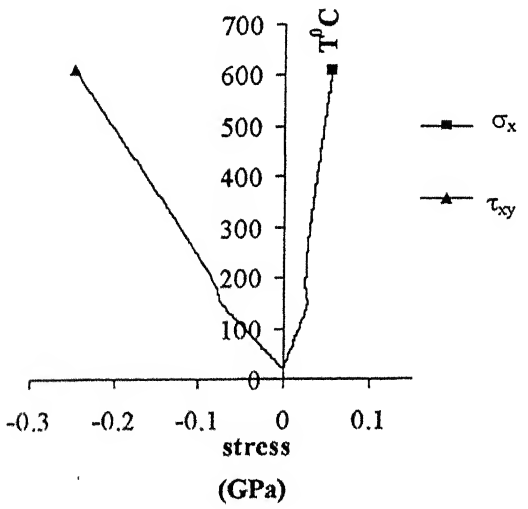

Fig. 3.12c Variation of stresses under temperature rise at node 1, layer 2

Figure 3.13a & b display σ_x and τ_{xy} distributions in the 15th layer at node point 1. At higher temperature, failure occurs at this point under combined loads. Here also σ_x and σ_y have the same values while the stress components τ_{xz} and τ_{yz} are neglegibly small. Graphs clearly show a substantial variation in stresses before and after buckling. In figs. 3.13a & b, the pattern of first three curves is significantly different from that of the rest.

The reason is that the temperature associated with each of these curves is less than the critical temperature, whereas for rest of the curves the plate is already in the post-buckling state due to the initial temperature rise. It may be noted that the nature of stresses at higher axial load is similar to the nature of the stresses under the temperature rise (see fig. 3.13a, b & c). It implies that, at the node under reference, at high temperatures the plate develops a stress state which is similar to that developed under high compressive loads. Because of this reason, the failure interaction curve in fig. 3.8 shows a steep variation (-ve slope) at higher temperature ranges.

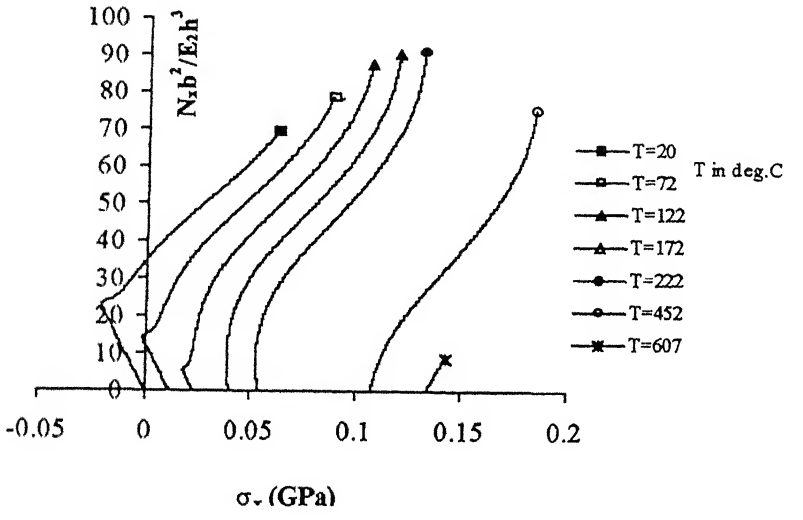

Fig. 3.13a Variation of stress σ_x at node 1, layer 15

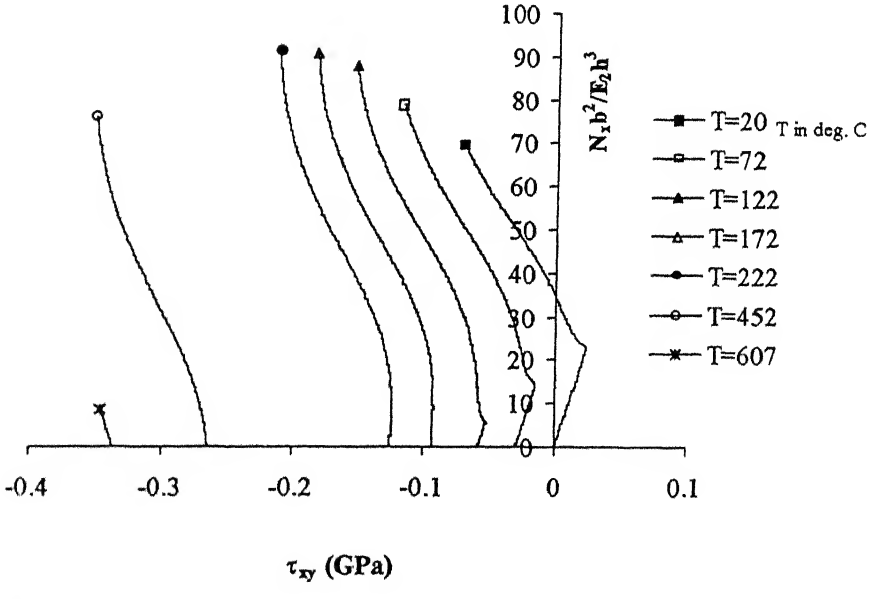

Fig. 3.13b Variation of stress τ_{xy} at node 1, layer 15

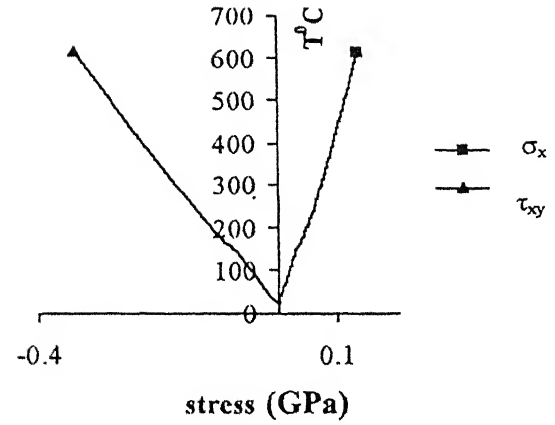

Fig. 3.13c Variation of stresses under temperature rise at node 1, layer 15

From the above discussion of failure under combined loads, it is clear that it is either the axial load (at low value of temperature) or the temperature (at elevated values of temperature) which decides the location and the mode of failure. A transition from failure due to the axial load to that by the thermal load is occurring at intermediate values of temperature and from fig 3.8 it is clear that the failure interaction curve shows a gradual transition in the gradient from +ve to -ve. Moreover, the curve shows distinct changes in its slope at different intervals.

As explained earlier, at initial temperatures the laminate failure occurs at corner point 1 of the 2nd lamina. During the transition in the gradient in fig. 3.8, the first-ply failure occurs at the center of the edges $x = 0, a$ (node 56,66) in laminae 13,15 & 16, the mode of failure being shear mode. It is to be noted that a change in slope of the failure interaction curve shows a change in failure characteristics and failure locations. It is observed that in intermediate temperature ranges, one or more than one of laminae from 10 to 16 (layer numbers) fails during loading. The distinct slope changes are associated with a change in the failure location, lamina and mode of failure.

3.3.4 Parametric study: effect of number of layers

A limited parametric study is carried out by considering the effect of number of layers in a symmetric quasi-isotropic laminate, $(45/-45/0/90)_{ns}$, by varying. n from 1 to 5. The analysis is performed by keeping the lamina thickness as constant (thickness of

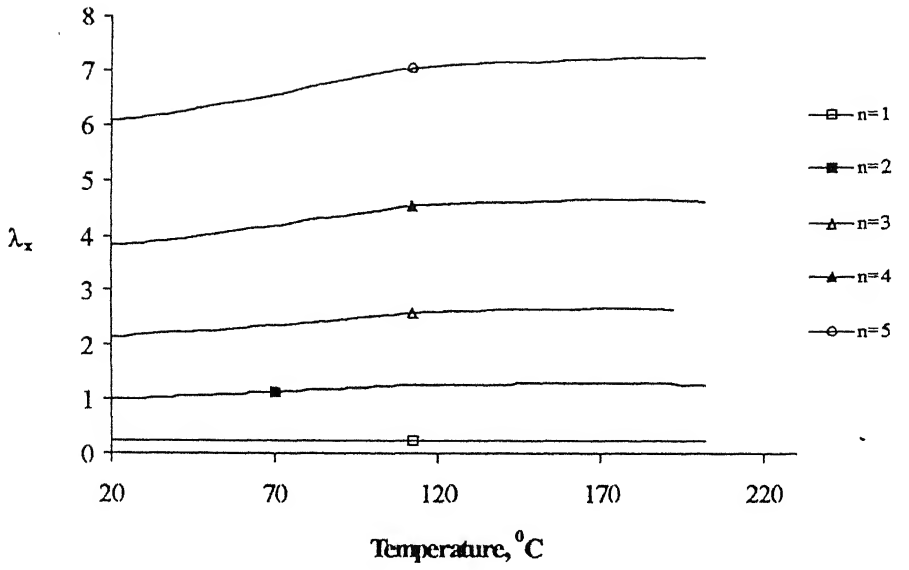

Fig. 3.14 First-ply failure envelopes for $(45/-45/0/90)_{ns}$ laminates under combined loading.

individual layer being 0.127 mm). Thermal dependent material properties are taken into consideration. First-ply failure interaction curves are obtained and shown in fig. 3.14. Graphs are plotted for λ_x versus temperature (T^0C). Here λ_x is the axial load normalized with buckling load for $(45/-45/0/90)_{2s}$ laminate at $T=20^0C$. The maximum temperature of 200^0C is considered as mentioned in section 3.3.1. It is clear that the first-ply failure strength of the laminate does not get reduced in the presence of a uniform temperature field.

CHAPTER 4

CONCLUDING REMARKS

The present investigation has been concerned with the post-buckling and failure response of symmetrically laminated composite plates subjected to combined temperature change and in-plane compressive edge load. The simply supported boundary condition, with edges free have in-plane movement in the normal direction and restrained against tangential displacement, has been adopted same in all cases. Laminates with temperature dependent and independent material properties have been analysed. Numerical studies have been made of the response characteristics, mainly stability and first-ply failure envelopes, of five different types of laminate lay-up that are subjected to combined loading. Results have been presented that show the variation in the laminate behavior for both temperature dependent and independent cases. An investigation of the stress-distributions has been made at laminate failure locations.

Based on numerical studies, the following observation seem to be justified :

- Stability interaction curves show a linear variation between the axial compression and the temperature rise for all lamination sequences considered. When the temperature dependency is accounted for, the laminates require lesser load to cause buckling as compared to the thermally independent case.

- Failure envelopes are of the similar nature for all laminates considered. The interaction curves are having a positive slope at smaller values of temperature, while at higher temperature ranges the curves are associated with a steep negative variation. In both cases, the failure takes place near the corner region, in the transverse mode.

- In the case of intermediate values of temperatures, the failure envelopes show a gradual change in the slope from + ve to –ve. Herein, failure characteristics show considerable changes when compared to that at the initial and the higher temperature ranges, in regard to the failure location and the nature of failure

- The failure interaction curve for the cross-ply laminate gives a lower bound, while that for the quasi-isotropic laminate yields an upper bound to first-ply failure envelopes.

- When temperature dependent material properties are accounted for, both stability and the first-ply failure envelopes (specially the latter) exhibit a distinct change.

- All the laminates do posses a considerable post-buckling strength in reserve. However, since the delamination aspect has not been considered, the decision to use this reserve strength would depend upon the maximum permissible transverse deflection consideration.

A few suggestions for further research are :

- Extensive parametric studies for a better understanding of the response characteristics of composite laminates with different boundary conditions and subjected to non-uniform temperature fields.

- Study of effects of geometric discontinuities in the form of cutouts and stiffeners.

- Enhancing the computational model by incorporating the heat transfer characteristics and inelastic material properties at higher temperature.

REFERENCES

Argyris, J. and Tenek, L. (1995), Post Buckling of Composite Laminate Under Compressive Loads and Temperature, *Comp. Methods in Appl. Mech. And Eng., 128, 49-80.*

Boley, B.A. and Weiner, J. J. (1960), *Theory of Thermal Stresses.* Wiley, New York, 1960.

Chen, L.W., Brunelle, E.J. and Chen, L.Y. (1982), Thermal Buckling of Initially Stressed Thick Plates, *ASME J. Mech. Design, 104(3), 557-64.*

Chen, J.K., Sun, C.T. and Chang, C.I. (1985), Failure Analysis of Graphite/Epoxy Laminate Subjected to Combine Thermal and Mechanic Loading, *J. of Composite Materials, 19, 408-423.*

Chen, L.W and Chen, L.Y. (1989), Thermal Postbuckling Analysis of Laminated Composite Plates by the Finite Element Method, *Composite Structures, 12, 257-270.*

Chen, L.W and Chen, L.Y. (1991), Thermal Postbuckling Behaviors of Laminated Composite Plates with Temperature-Dependent Properties, *Composite Structures, 19, 267-283.*

Chia, C-Y. (1980), *Nonlinear Analysis of Plates*, Mc Graw-Hill, Int. Book Company.

Chia, C-Y. (1988), Geometrically Nonlinear Behavior of Composite Plates: A Review, *Appl. Mech. Rev., 41(12), 439-451.*

Fung, Y.C. (1965), *Formulations of Solid mechanics*, Prentice Hall.

Huang, N.N. and Tauchert, T.R. (1988a), Postbuckling Response of Anti-symmetric Single-ply Laminates to Uniform Temperature Loading, *Acta Mechanica, Vol.72, pp. 173-183.*

Huang, N.N. and Tauchert, T.R. (1988b), Large Deformation of Anti-symmetric Angle-ply Laminates Resulting from Nonuniform Temperature Loading, *J. of Thermal Stresses, 11, 287-297.*

Huang, N.N. and Tauchert, T.R. (1991), Large Deflections of Laminated Cylindrical and Doubly-Curved Panels under Thermal Loading, *Computers and Structures, 41(2), 303-312.*

Hinton, E., Razzaque, A., Zienkiewicz, O.C. and Davis, J.D. (1975), A Simple Finite Element Solution for plates of Homogeneous, Sandwich and Cellular Construction, *Proc. Inst. Civ. Engrs.* Part-2, 59, 43-65.

Jones, R.M. (1975), *Mechanics of Composite Materials*, Scripta Book Co., Washington

Kumar, A. and Dixit, N.K. (1994), Thermally Induced Nonlinear Response of Cross-ply Laminates, *J. Aero. Soc. of India,* 46,116-121.

Librescu, L. and Souza, M.A. (1993), Post-buckling of Geometrically Imperfect Shear-deformable flat Panels Under Combined Thermal and Compressive Edge Loadings, *ASME J. Mech., 60(2), 526-33.*

Mindlin, R.D. (1951), Influence of Rotatory Inertia and shear on Flexural Motions of Isotropic, Elastic Plates, *J. of Appl. Mech.,* 18. 31-38.

Mayers, C.A. and Hyer, M.W (1992), Thermally Induced Geometrically Nonlinear Response of Symmetrically Laminated Composite Plates, *Composite Engineering, 2(1), 3-20.*

Noor, A.K, and Burton, W.S. (1991), Predictor-Corrector analysis for Thermal Buckling Analysis of Multilayered Composite Plates, *Computer and Structures, Vol 40, No.5, 1071-1084.*

Noor, A.K. and Peters, J.M. (1992) Thermomechanical Buckling of Multilayered Composite Plates, *ASCE. J. Eng Mech., 118(2), 351-66.*

Noor, A.K., Starnes, J.H. and Peters, J.M. (1993), Thermomechanical Buckling and Postbuckling of Multilayerd Composite Panels, *Composite Structures, 23(3),91-104.*

Pugh, E.D.L., Hinton, E. and Zienkievicz, O.C. (1978), A Study of Quadrilateral Plate Bending Elements with Reduced Integration. *Int. J. Num. Meth. Eng,* 12, 1059-1079.

Reddy, J.N. and Pandey, A.K. (1987), A First-ply Failure Analysis of Composite Laminates, *Computers and Structures*, 25, 371-393.

Reddy, Y.S.N. and Reddy, J.N. (1992), Linear and Non-linear Failure Analysis of Composite laminates with Transverse Shear, *Composite Science and Technology,* 44, 277-255.

Sadovsky, Z. (1993), Buckling of compressed rectangular plates at non-uniformly elevated temperatures, *Thin Walled Struct., 15(2), 95-107*

Shen, H. and Lin, Z-Q. (1995), Thermal Post-buckling Analysis of Imperfect Laminated Plates, *Computers and Structures,* 57(3), 533-540.

Shen, S.H. and Sun, G. (1996), Thermomechanical Postbuckling Analysis of Imperfect laminated Plates on Two-parameter Elastic foundations, *Composite Structures, 34 , 325-338.*

Singh, S.B. (1996), Postbuckling Response, Strength and Failure of Symmetric Laminates, *Doctoral Thesis*, Indian Institute of Technology Kanpur, India.

Singh, S.B., Kumar, A and Iyengar, N.G.R. (1997), Progressive Failure of symmetrically Laminated Plates under Uni-axial Compression, *Structural Eng. and Mech.*, 5(4), 433-450.

Srikanth, G. (1997), Thermally-induced Nonlinear Response of Laminated plates, *M.Tech. Thesis, Department of Civil Engineering, I.I.T. Kanpur,* India

Tauchert, T.R. (1991), Thermally Induced Flexure, Buckling and Vibration of Plates, *Review of Thermal Stresses, 44(8), 347-360.*

Tsai, S.W. and Wu, E.M. (1971), A General Theory of Strength for Anisotropic Materials, *J. of Composite Materials,* 5,58-80.

Zienkiewicz, O.C. (1978), *The Finite Element Method,* Mc Graw-Hill Book Company, Newyork.

Zienkiewicz, O.C. (1992), *The Finite Element Method,* Mc Graw-Hill Book Company, Newyork.

APPENDIX I

The thermo-mechanical stress-strain relations for the k^{th} lamina of the laminate in the principal material directions can be expressed as (Jones, 1975)

$$\begin{bmatrix} \sigma_1 \\ \sigma_2 \\ \tau_{12} \\ \tau_{23} \\ \tau_{13} \end{bmatrix} = \begin{bmatrix} C_{11} & C_{12} & 0 & 0 & 0 \\ C_{21} & C_{22} & 0 & 0 & 0 \\ 0 & 0 & C_{33} & 0 & 0 \\ 0 & 0 & 0 & C_{44} & 0 \\ 0 & 0 & 0 & 0 & C_{55} \end{bmatrix} \begin{Bmatrix} \varepsilon_1 - \alpha_1 \Delta T \\ \varepsilon_2 - \alpha_2 \Delta T \\ \gamma_{12} \\ \gamma_{23} \\ \gamma_{13} \end{Bmatrix}$$

and σ_3 is given in the following section.

$$\sigma_3 = C_{13}\varepsilon_1 + C_{23}\varepsilon_2$$

where

$$C_{11} = \frac{E_1}{1 - \nu_{12}\nu_{21}}; \qquad C_{12} = C_{21} = \frac{\nu_{12}E_2}{1 - \nu_{12}\nu_{21}}$$

$$C_{22} = \frac{E_2}{1 - \nu_{12}\nu_{21}}; \qquad C_{33} = G_{12}; \qquad C_{44} = G_{23}$$

$$C_{55} \quad G_{13}; \qquad \frac{\nu_{21}}{E_2} = \frac{\nu_{12}}{E_1}$$

$$C_{13} = \frac{\nu_{31} + \nu_{21}\nu_{32}}{E_2 E_3 \Delta} = \frac{\nu_{13} + \nu_{12}\nu_{23}}{E_1 E_2 \Delta}$$

$$C_{23} = \frac{\nu_{32} + \nu_{12}\nu_{31}}{E_1 E_3 \Delta} = \frac{\nu_{23} + \nu_{21}\nu_{13}}{E_1 E_2 \Delta}$$

$$\Delta = \frac{1 - \nu_{12}\nu_{21} - \nu_{23}\nu_{32} - \nu_{31}\nu_{13} - 2\nu_{21}\nu_{32}\nu_{13}}{E_1 E_2 E_3}$$

and $[\sigma_1, \sigma_2, \sigma_3, \tau_{12}, \tau_{23}, \tau_{13}]^T$ are the stress components and $[\varepsilon_1, \varepsilon_2, \varepsilon_3, \gamma_{12}, \gamma_{23}, \gamma_{13}]^T$ are the total strain components referred to the lamina coordinates (1-2-3). The C_{ij} are the elastic constants of the k^{th} lamina; E_i are the Young's moduli of elasticity in the i^{th} direction, ν_{ij} are the Poisson's ratios that give strain in the j^{th} direction due to stress in the i^{th} direction and G_{12}, G_{23} and G_{13} are the shear moduli principal plane direction 1-2, 2-3, and 1-3, respectively. The α_1 and α_2 thermal expansion coefficients in the material directions 1 and 2 respectively and ΔT is the temperature change.

The plane stress reduced elastic constants in the structural axis (laminate axis), $Q'_{ij}s$ of the k^{th} lamina, are

$$Q_{11} = C_{11}c^4 + (2C_{12} + 4C_{33})s^2c^2 + C_{22}s^4$$

$$Q_{12} = (s^4 + c^4)\,C_{12} + (C_{11} + C_{22} - 4C_{33})s^2c^2$$

$$Q_{13} = (C_{11} - C_{12} - 2C_{33})\,c^3s + (C_{12} - C_{22} + 2C_{33})s^3c$$

$$Q_{22} = C_{11}s^4 + (2C_{12} + 4C_{33})s^2c^2 + C_{22}c^4$$

$$Q_{23} = (C_{11} - C_{12} - 2C_{33})\,s^3c + (C_{12} - C_{22} + 2C_{33})sc^3$$

$$Q_{66} = C_{11}s^4 + (C_{11} - 2C_{12} + C_{22} - 2C_{33})s^2c^2 + (c^4 + s^4)C_{33}$$

$$Q_{44} = C_{44}c^2 + C_{55}s^2$$

$$Q_{55} = C_{44}s^2 + C_{55}c^2$$

Where $Q_{ij} = Q_{ji}$, $c = cos\alpha$, $s = sin\alpha$ and α = lamina orientation which is measured positive in the ani-clock wise direction.

APPENDIX II

Substituting the eqn. (2.81) in eqn. (2.87) , K_T can be written as

$$\int_A [B_0]^T \begin{bmatrix} \frac{\partial N_x}{\partial a_1} & \frac{\partial N_x}{\partial a_2} & \cdots & \frac{\partial N_x}{\partial a_m} \\ \frac{\partial N_y}{\partial a_1} & \frac{\partial N_y}{\partial a_2} & \cdots & \frac{\partial N_y}{\partial a_m} \\ \frac{\partial N_{xy}}{\partial a_1} & \frac{\partial N_{xy}}{\partial a_2} & \cdots & \frac{\partial N_{xy}}{\partial a_m} \end{bmatrix} dA +$$

$$\int_A [B_b]^T \begin{bmatrix} \frac{\partial M_x}{\partial a_1} & \frac{\partial M_x}{\partial a_2} & \cdots & \frac{\partial M_x}{\partial a_m} \\ \frac{\partial M_y}{\partial a_1} & \frac{\partial M_y}{\partial a_2} & \cdots & \frac{\partial M_y}{\partial a_m} \\ \frac{\partial M_{xy}}{\partial a_1} & \frac{\partial M_{xy}}{\partial a_2} & \cdots & \frac{\partial M_{xy}}{\partial a_m} \end{bmatrix} dA +$$

$$\int_A [B_s]^T \begin{bmatrix} \frac{\partial Q_x}{\partial a_1} & \frac{\partial Q_x}{\partial a_2} & \cdots & \frac{\partial Q_x}{\partial a_m} \\ \frac{\partial Q_y}{\partial a_{21}} & \frac{\partial Q_y}{\partial a_2} & \cdots & \frac{\partial Q_y}{\partial a_m} \end{bmatrix} dA +$$

$$\int_A [B_s]^T \begin{bmatrix} N_x \frac{\partial}{\partial a_1}\left(\frac{\partial w}{\partial x}\right) + N_{xy} \frac{\partial}{\partial a_1}\left(\frac{\partial w}{\partial y}\right) & \cdots & N_x \frac{\partial}{\partial a_m}\left(\frac{\partial w}{\partial x}\right) + N_{xy} \frac{\partial}{\partial a_m}\left(\frac{\partial w}{\partial y}\right) \\ N_y \frac{\partial}{\partial a_1}\left(\frac{\partial w}{\partial x}\right) + N_{xy} \frac{\partial}{\partial a_1}\left(\frac{\partial w}{\partial y}\right) & \cdots & N_y \frac{\partial}{\partial a_m}\left(\frac{\partial w}{\partial x}\right) + N_{xy} \frac{\partial}{\partial a_m}\left(\frac{\partial w}{\partial y}\right) \end{bmatrix} dA \quad \text{(A2.1)}$$

It can be shown that

$$\frac{\partial}{\partial \{a\}^T}\{\overline{N}\} = [A][B_0] + [B][B_b] \quad \text{(A2.2a)}$$

$$\frac{\partial}{\partial \{a\}^T}\{\overline{M}\} = [B][B_0] + [D][B_b] \quad \text{(A2.2b)}$$

$$\frac{\partial}{\partial\{a\}^T}\{Q\} = [E][B_s] \tag{A2.2c}$$

$$\frac{\partial}{\partial a_i}\left(\frac{\partial w}{\partial x}\right) = \begin{cases} \dfrac{\partial N_i}{\partial x} & \text{for } w_i \rightarrow \text{nodal degree of freedom.} \\ 0 & \text{for other degrees of freedom} \end{cases} \tag{A2.2d}$$

$$\frac{\partial}{\partial a_1}\left(\frac{\partial w}{\partial x}\right) = \begin{cases} \dfrac{\partial N_i}{\partial y} & \text{for } w_i \rightarrow \text{nodal degree of freedom.} \\ 0 & \text{for other degrees of freedom} \end{cases} \tag{A2.2e}$$

Substituting eqns. (A2.2) in eqn. (A2.1) and reàrranging gives the expression for K_T as shown in eqn (2.88)